Peroxydisulfate activation process on copper oxide: Cu(III) as the predominant selective intermediate oxidant for phenol and waterborne antibiotics removal

Chan Li, Vincent Goetz, Serge Chiron

Peroxydisulfate activation process on copper oxide: Cu(III) as the predominant selective intermediate oxidant for phenol and waterborne antibiotics removal

Chan Li[1], Vincent Goetz[2] and Serge Chiron[1*]

[1]UMR HydroSciences Montpellier, Montpellier University, IRD, 15 Ave Charles Flahault 34093 Montpellier cedex 5, France

[2]PROMES-CNRS UPR 8521, PROcess Material and Solar Energy, Rambla de la Thermodynamique, 66100 Perpignan, France

*Corresponding author: Tel: + 33 - 411759415; Fax: + 33 - 411759414; e-mail address: serge.chiron@umontpellier.fr

GRAPHICAL ABSTRACT

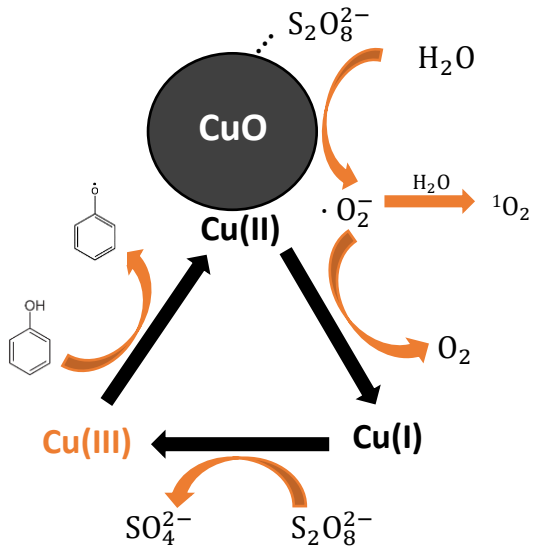

Abstract

In this study, activated peroxydisulfate (PDS) by micrometer copper oxide (CuO) particles effectively degraded phenol and several antibiotics in water. Cupryl ion (Cu(III)) was proposed for the first time to be the predominant reactive species accounting for contaminants degradation in the CuO/PDS oxidation system. Singlet oxygen was also heavily produced from the superoxide radical anion ($^{\bullet}O_2^-$) decomposition was found to be but slightly involved in the degradation since it was rapidly quenched by water. Transformation pathways of phenol and several antibiotics were elucidated. The proposed mechanism mainly involved the generation of $^{\bullet}O_2^-$ resulting from an outer-sphere surface PDS complexation which prompted the reduction of Cu(II) to Cu(I). Cu(I) was oxidized in Cu(III) by PDS or H_2O_2 and was reduced to Cu(II) by a one-electron oxidation of contaminants so that the catalytic effect involved alternate oxidation and reduction of copper. As the degradation process did not rely on sulfate or hydroxyl radical, chloride and bicarbonate ions showed no effect on phenol degradation, while sulfate ions and humic acid slightly hindered phenol degradation probably due to their sorption on CuO. Interestingly, the copper leaching from CuO was significantly limited to < 500 µg/L in wastewater. These findings indicated the potential applicability of CuO/PDS system for electron-rich compounds degradation including antibiotics due to good catalyst stability against time.

Keywords: copper oxide; peroxydisulfate; cupryl ion; non-radical mechanism; transformation pathways; antibiotics.

1. Introduction

The success of many advanced oxidation processes (AOPs) based on persulfate (PS) including peroxydisulfate (PDS) and peroxymonosulfate (PMS) for water treatment relies on the strong oxidizing power of the generated free radical species (hydroxyl ($^{\bullet}OH$) E^0 1.9−2.7 V and sulfate ($SO_4^{\bullet-}$) E^0 2.5−3.1 V) towards a broad spectrum of recalcitrant organic contaminants and towards pathogens [1,2]. However, radical-based PS activation requires the input of energy mainly in the form of light, ultrasound and heat which elevates the operational costs of treatments [3,4]. Consequently, among the different strategies to activate PS, transition metals (Fe^{2+}, Cu^{2+}, Mn^{2+}), their oxides (Fe_3O_4, CuO, MnO_2), and bimetallic composites ($CuFe_2O_4$, CuO−Fe_3O_4, $Mn_{1.8}Fe_{1.2}O_4$, etc.) and supported metal oxides (CuOMgO-Fe_3O_4, CuO-Al_2O_3) have been recognized as the most cost-efficient approaches [4–6]. Iron oxides received particular attention to heterogeneously activate PS, because they are not consumed during the activation, can work at neutral pH, and no additional energy is required [7,8]. However, the low efficiency of present heterogeneous activation processes in terms of long contact time (usually in days) and high PS dose requested (over 100 times higher than the pollutant concentration) is still a major limitation for its industrial application [9]. Consequently, copper, mainly in the forms of pure copper oxides (e.g., CuO or Cu_2O) [10,11], bimetallic oxides (e.g., $CuFe_2O_4$, $CuFeO_2$) [12,13] and different materials supported copper oxides (e.g., CuO supported on alumina, or CuO coated on ceramic hollow fiber membrane) [6,14] has obtained increasing attention because of their higher efficiency than iron oxides to activate PS with still relatively low toxicity of Cu^{2+} ion in case of leaching. Indeed, an upper Cu^{2+} concentration limit of 2.0 mg/L is admitted in drinking water and Cu^{2+} is not regarded as a potential carcinogen [15].

Processes relying on radical-based mechanisms undergo efficiency losses in organic-rich wastewater such as domestic wastewater due to the competing organic/inorganic constituents of water [4] and due to the difficulty in the regeneration of active sites on the surface of the catalyst due to the energetically unfavorable Cu redox cycle. In particular, the oxidation by $SO_4^{\bullet-}$ favors the direct electron abstraction and can transform some anions (e.g., Cl^- and NO_2^-) into their corresponding radicals potentially leading to troublesome chlorinated and nitrated transformation products (TPs) [4,16]. More recently, mild non-radical PS activation mechanisms have been also suggested to limit the formation of these hazardous TPs. In contrast to radical-based processes, the non-radical oxidative pathway is much more selective, accounting for the only removal of electron-rich organic contaminants (e.g., phenols and anilines) [11,17,18]. In addition, the non-radical pathway requires a small amount of oxidant and is less influenced by the competing organic/inorganic constituent of the water. Three major mechanisms have been proposed for the non-radical pathway including the involvement of 1) oxidant surface metastable complexes on CuO particles, 2) superoxide radical anion ($^{\bullet}O_2^-$) and singlet oxygen ($^1O_2$) and 3) the high valent cupryl ion oxidant symbolized by Cu^{3+} in solution and Cu(III) in its solid form. Surface activated complexes result from the interaction between CuO and PS through an outer-sphere surface complexation [11,17]. PS is thought to function as a two-electrons transfer oxidant that directly accepts electrons from an organic contaminant through an electron shuttle material leading to sulfate anions (SO_4^{2-}) release. Certain recent

studies have reported the occurrence $^1O_2$ as another type of non-radical process as previously reported in the CuOs/PS system [18,19]. $^{\bullet}O_2^-$ might function as a precursor for the generation of $^1O_2$ through $^{\bullet}O_2^-$oxidation or disproportionation reactions. The $^1O_2$ based systems are well-known for their resistance to background substances in the water matrix but have been regarded to be poorly efficient because $^1O_2$ is rapidly quenched by water [20]. Cu(III) has been also suggested to be the working oxidant in the copper involved activated PS processes [21–23]. The generation of Cu in a highly electron deficient state offers the highest redox potential for PS activation (Cupric ion symbolized by Cu^{2+} in solution and Cu(II) in its solid form, E^0Cu(III)/Cu(II) = 2.3 V,) but Cu(III), as an unstable species and an one-electron oxidant, might also directly oxidize electron-rich organic contaminants [24] or decompose into $^{\bullet}$OH, depending on the water pH value [25].

Consequently, using CuO, there is still a great deal of uncertainty concerning the identification of reactive species since all the different above mentioned pathways have been reported in the literature from the radical pathway, the surface bound complex, the $^1O_2$ pathway and the high-valent metal-induced Cu(III) oxidation pathway during PS activation. The mechanisms behind the identification of reactive species and transformation of organics still need further exploration. This is the main contribution of this work by taking PDS as the working oxidant because PDS is a more promising oxidant than PMS for potential applications due to a better chemical stability during transport and storage, a lower cost and a longer half-life [26]. Specific objectives of this work include: (i) kinetic studies, (ii) identification of reactive species by using scavengers, (iii) identification of TPs by liquid chromatography-high resolution-mass spectrometry (LC-HRMS) and elucidation of transformation pathways, (iv) investigating the effect of operating parameters, and (v) investigating the practical applicability on the removal of several antibiotics. Phenol was selected as one probe organic contaminant because of its well-known reactions with common radical and non-radical species and the applicability of the CuO/PDS system was investigated by using several antibiotics (i.e. cephalexin (CFX), ciprofloxacin (CIP), clarithromycin (CLA) and sulfamethoxazole (SMX)) of environmental relevance.

2. Material and methods

2.1 Chemicals

Micrometer copper oxide particles (CuOμm, 44 μm, 97%) were purchased from Alfa Aesar (Kandel, Germany). Nanometer copper oxide (CuOnm, < 50 nm), iron (II, III) oxide (Fe_3O_4), cuprospinel ($CuFe_2O_4$), ammonium molybdate ($(NH_4)_6Mo_7O_{24}\cdot 4H_2O$), anisole (> 99%), benzoic acid (> 99%), benzotriazole (> 98%), catechol (> 99%), CFX (> 99%), CIP (> 98%), CLA (> 99.5), furfuryl alcohol (FFA, > 99%), humic acids sodium salt (technical grade), hydrochloric acid (HCl, 37%), hydroxyquinone (HQ, > 99%), nitrobenzene (NB, > 98%), Oxone ($KHSO_5\cdot 0.5KHSO_4\cdot 0.5K_2SO_4$), *p*-benzoquinone (BQ, > 98%), phenol (> 99%), salicylic acid (> 99%), sodium azide (NaN_3, > 99.5%), SMX (> 99%), sulfuric acid (H_2SO_4, 98%), sodium bicarbonate ($NaHCO_3$), sodium hydroxide (NaOH), starch solution, 4-

hydroxybenzoic acid (> 99%) and 4-phenoxyphenol (> 99%) were purchased from Sigma-Aldrich (Saint Quentin Fallavier, France). CuO supported on alumina ($CuO@Al_2O_3$), potassium iodide (KI), and potassium periodate (KIO_4) were purchased from Honeywell (Germany). Copper sulfate pentahydrate ($CuSO_4 \cdot 5H_2O$), potassium persulfate ($K_2S_2O_8$) and tris(hydroxymethyl)aminomethane (Tris) were purchased from Merck KGaA (Germany). Acetonitrile (HPLC grade), methanol (MeOH, HPLC grade) and sodium chloride (NaCl) were purchased from Carlo Erba reagents (France). All solutions were prepared with ultrapure water obtained from a Milli-Q Plus system (Millipore, Bedford, MA). Stock solutions of phenol (1000 ppm) and PDS (100 mM) were prepared in ultrapure water.

2.2 Characterization of CuO

CuOμm, CuOnm, Fe_3O_4, $CuFe_2O_4$, $CuO@Al_2O_3$ were used as received without any further purification. Only CuOμm underwent further characterization as it was selected for deeper investigation. The surface morphology and chemical composition of CuOμm were analyzed using a scanning electron microscope (SEM). To identify its crystal structure, X-ray diffraction (XRD) analyses were performed at room temperature using a PANalytical XPert Pro diffractometer (CuKα radiation, λ= 0.15418 nm). XRD measurements of θ-θ symmetrical scans were made over an angular range of 10 to 80°. BET surface area and average pore size were analyzed by the N_2 adsorption method.

2.3 Experimental procedures

Batch experiments were conducted in 100 mL glass serum bottles under continuous shaking by roller mixer (STUART® SRT9D, UK) at 60 rpm and using 200 mM Tris buffer adjusted at pH 7 with HCl or NaOH. The use of phosphate and borate buffers were discarded to set the pH at 7 or slightly basic pH because phosphate is a strong coordinate for transition metals and particularly Cu^{2+} while PS activation by borate has been reported [27]. Typically, compound, metal oxides, and PDS were sequentially added into the bottles to reach initial concentrations of 20 mg/L (0.213 mM), 10 g/L and 1 mM, respectively. Sample aliquots (5 mL) were taken at predetermined times and filtered through 0.45 μm membrane filters, and then stored in 6 mL glass tubes at 4 °C before analysis. Control experiments without the addition of metal oxide or oxidant were also performed under the same experimental conditions. High concentration of scavengers (usually more than 100 times of phenol concentration), like MeOH, anisole, NB, BQ, FFA, NaN_3, neocuproine and hydroxylamine were added in the CuO/PDS system, respectively to probe the generated reactive oxidant species. Results are presented as an average of two experiments.

2.4 Analytical methods

Phenol, BQ, and HQ were quantified by LC with a diode-array detector at λ = 280, 244 and 254 nm, respectively using an Agilent ZORBAX Eclipse XDB C_8 column (150 × 3 mm i.d., 3.5 μm particle size) for kinetic studies. The separation was performed using an isocratic mode of elution with a mobile phase composed of 0.1% formic acid in Milli-Q water and acetonitrile at a volume ratio of 50/50 for phenol and 90/10 for BQ and HQ. The flow rate was set at 0.5 mL/min. TPs were detected by LC-HRMS composed of a Dionex Ultimate 3000 liquid

chromatograph equipped with an electrospray source and a Exactive Orbitrap mass spectrometer (Thermo Fisher Scientific, Les Ulis, France) operated in full scan MS (mass range m/z 50-900) and using an Agilent ZORBAX Eclipse XDB C_{18} plus column (150 × 2.1 mm i.d., 3.5 μm particle size). Phenol TPs detected in negative ionization mode and the LC gradient of Milli-Q water (solvent A) and acetonitrile (solvent B) was as follow: 0-1.5 min, 98% A; 11.25 min, 55% A; 12.75 min, 30% A; 13.0-20 min, 98% A. The flow rate was 0.3 mL/min. The energy collisional dissociation was set to 20 eV and a drying gas temperature of 275 °C was used. Quantification of phenoxyphenol dimers were carried out by external calibration using 4-phenoxyphenol as available analytical standard. Antibiotic TPs detected in positive ionization mode and the LC gradient of Milli-Q water with 1% acetonitrile and 0.1% formic acid (solvent A) and acetonitrile with 1% Milli-Q water and 0.1% formic acid (solvent B) was as follow: 0-5 min, 95% A; 15-20 min, 5% A; 21-30 min, 95% A. The flow rate was 0.15 mL/min. The energy collisional dissociation was set to 20 eV and a drying gas temperature of 300 °C was used.

Analysis of PDS. PDS was determined by using a UV-Vis spectrophotometer (Shimadzu, Japan) following the protocol developed by Liang et al., [28]. Briefly, the method consisted in analyzing adsorption spectra of mixed solutions of 1 mL sample, 1 mL 60 mM $NaHCO_3$, and 1 mL 600 mM KI in a quartz cuvette at $\lambda = 352$ nm.

Analysis of hydrogen peroxide. H_2O_2 was determined by using UV-Vis spectrophotometry following the protocol developed by Graf and Penniston [29]. Briefly, the method consisted in analyzing adsorption spectra of mixed solutions of 2 mL 50 mM HCl, 0.2 mL 1 M KI, 0.2 mL 1 mM ammonium molybdate in 0.5 M H_2SO_4, 0.2 mL 50 g/L starch solution and 0.2 mL sample in a quartz cuvette at $\lambda = 570$ nm.

Analysis of Cu(III). The Cu(III) periodate complex was analyzed by UV-Vis spectrophotometry following the protocol of Wang et al., [23]. Briefly, KIO_4 (4 g/L) was added in the basic solution (pH = 13) consisted of CuO (10 g/L) and PDS (1 mM) and NaOH. Samples (3 mL) were filtered through 0.45 μm membrane filters after 5 min reaction and the 300-600 nm UV/Vis absorption spectra of the filtered solution were recorded.

3. Results and discussion

3.1 Characterization of CuO

Representative SEM image and XRD diffraction pattern of the investigated micrometer CuO are shown in Fig. 1. The SEM image shows that CuO particles were irregularly shaped crystals with mean diameters of about 44 μm. The XRD pattern of CuO matched well with the standard XRD pattern of copper oxide (ICDD 01-089-5897) and indicated that CuO was a monoclinic system with 100% crystallinity. The specific surface area was found to be 0 m^2g^{-1} and there was no porosity.

3.2 PDS activation by CuO – batch experiments

First, the degradation of PDS and phenol (see Fig. S1 in Supporting Material) with three different catalysts (i.e., CuO, Fe_3O_4 and $CuFe_2O_4$) has been compared to demonstrate the higher

reactivity originated from CuO for the degradation of phenol and the oxidant consumption. Then, the same comparison was conducted among different types of CuO (i.e., CuOnm, CuOμm, CuO supported on alumina) (see Fig. S2). CuOμm was selected in this work because of its high reactivity for phenol degradation, and because micro-sized particles allow for easy catalyst separation and recovery, which is of great importance in practical applications.

At neutral pH (7.0 ± 0.3), PDS alone could not degrade phenol and CuO alone could not adsorb phenol. Interestingly, the phenol degradation reached 100% in 15 min in presence of CuO and PDS (Fig. 2a). Phenol degradation fitted a first-order kinetic model with an apparent degradation kinetic rate constant (k_{obs}) of 0.32 min^{-1}. The corresponding PDS decomposition is shown in Fig. 2b. The presence of catalysts without an organic component decomposed PDS to a significant extent. The lack of decrease or increase in the decomposition of PDS after phenol addition ruled out the mediator role of the catalysts through the direct transfer of electrons between phenol and PDS. As previously reported [11,17], the interaction between CuO and PDS likely occurred through an outer-sphere surface complexation. Due to the positively charged CuO and the negatively charged PDS at neutral pH, strong electrostatic interactions and adsorption of PDS on the CuO surface were anticipated. However, this adsorption process could not be quantified due to the simultaneous PDS reactivity on the CuO particle surface. Besides, since Cu^{2+} ions neither catalyzed PDS activation nor degraded phenol (Fig. 2a and b), the effects of Cu^{2+} leaching could be ruled out and the predominant role of heterogeneous PDS activation could be stated. Cu^{2+} was previously reported to donate one electron to PDS, thus inducing PDS decomposition into sulfate anion and sulfate radical. However, this process is very slow, making effective degradation of water pollutants nearly impossible except for specific compounds, which can directly complex with Cu^{2+} [21,30]. The stoichiometric efficiency (η), defined as the number of moles of phenol oxidized for every mole of PDS activated ($\eta = \Delta[\text{phenol}] / \Delta[S_2O_8^{2-}] \times 100\%$) was also calculated. 45-50% was found to be the maximum value that could be obtained. This meant that two moles of PDS was needed to degrade one mole of phenol on average.

3.3 Identification of reactive species

A central question was the identification of the active oxidant species in the chemical transformation of the probe compound at neutral pH. It has been suggested that $^{\bullet}OH$, $SO_4^{\bullet-}$, $^{\bullet}O_2^-$, $^1O_2$ and probably Cu(III) are formed in CuO catalyzed PDS processes [17,19,31,32]. MeOH was first used to investigate a possible formation of radical species. MeOH reacts with $^{\bullet}OH$ and $SO_4^{\bullet-}$ with nearly the same rate (k_2 (MeOH, $SO_4^{\bullet-}$) = 1 x10^7 $M^{-1}s^{-1}$, [33]), k_2 (MeOH, $^{\bullet}OH$) = 5 x10^8 $M^{-1}s^{-1}$, [25]) and can theoretically be used to trap these radicals. The inhibitory effect of MeOH was limited as k_{obs} only change from 0.32 min^{-1} to 0.18 min^{-1} after applying an excess amount of MeOH (see Table 1 and Fig. S3a). This result confirmed earlier findings that the CuO/PDS system did not predominantly rely on radical mechanisms. The lack of ability for MeOH to scavenge surface bound radicals might also account for the observed small inhibition in phenol degradation [13]. To scavenge the surface bound radicals, inhibitors that can interact onto the CuO surface and can lead to the subsequent occupation of activated sites are needed [34]. For this purpose, the addition of anisole which can complex with Cu(II) [35] and react

with $^{\bullet}OH$ and $SO_4^{\bullet-}$ (k_2 (anisole, $SO_4^{\bullet-}$) = 7.8×10^9 $M^{-1}s^{-1}$, [36]; k_2 (anisole, $^{\bullet}OH$) = 4.9×10^9 $M^{-1}s^{-1}$, [37]) was tested. Similarly, anisole had a very limited inhibitory effect (k_{obs} = 0.24 min^{-1}, Table 1 and Fig. S3a), confirming the limited implication of radicals in solution and/or adsorbed on CuO surface in the phenol degradation process.

To discriminate against the different radicals (i.e., $^{\bullet}OH$ and $SO_4^{\bullet-}$), NB as a specific $^{\bullet}OH$ quencher (k_2 (NB, $^{\bullet}OH$) = 3.2×10^9 $M^{-1}s^{-1}$, [38]; k_2 (NB, $SO_4^{\bullet-}$) < 10^6 $M^{-1}s^{-1}$, [39]) was applied. As shown in Table 1 and Fig. S3a, the no NB effect on the phenol degradation kinetic (k_{obs} = 0.32 min^{-1}) excluded the involvement of $^{\bullet}OH$ in the system. This result validated the selection of Tris buffer to set the pH at 7 because it is known that Tris quickly reacts with $^{\bullet}OH$ to generate formaldehyde with a second-order rate constant of 1.1 x10^9 $M^{-1}s^{-1}$ [40]. The observed difference between k_{obs} in presence of anisole or NB could only be ascribed to some generated $SO_4^{\bullet-}$ radicals. BQ as a known scavenger for $^{\bullet}O_2^-$ (k_2 (BQ, $^{\bullet}O_2^-$) = 8×10^9 $M^{-1}s^{-1}$, [41]) was also applied. The degradation of phenol was totally inhibited, which demonstrated the predominant role of $^{\bullet}O_2^-$ in CuO/PDS system. Besides, $^{\bullet}O_2^-$ reacts relatively rapidly with Cu^{2+} and H_2O (k_2 (Cu^{2+}, $^{\bullet}O_2^-$) 8×10^9 $M^{-1}s^{-1}$; k_2 (H_2O, $^{\bullet}O_2^-$) = 1.0×10^5 $M^{-1}s^{-1}$; [42]) compared with phenol (k_2 (phenol, $^{\bullet}O_2^-$) = 5.8×10^2 $M^{-1}s^{-1}$, [43]). Consequently, the major role of $^{\bullet}O_2^-$ was not to degrade phenol but might function as precursors to reduce Cu^{2+} to Cu^+ and to generate $^1O_2$ along with H_2O_2 generation through bimolecular dismutation.

To confirm this point, the formation of Cu^+, $^1O_2$, and H_2O_2 was examined individually. To verify Cu^+ formation, neocuproine as a specific Cu^+ chelating agent and trace hydroxylamine as a reductant to promote Cu^{2+} conversion to Cu^+ were selected to apply in the CuO/PDS system [23,44]. Neocuproine was prepared in presence of methanol (4.9 M) due to its poor water solubility. Neocuproine hindered the degradation of phenol with k_{obs} = 0.05 min^{-1} and trace hydroxylamine slightly promoted the degradation of phenol with k_{obs} = 0.40 min^{-1} (Table 1 and Fig. S3b). Both results indicated that Cu^+ most likely played an important role in the copper redox cycle in the presence of PDS to generate reactive species.

$^1O_2$ exhibits highly selective oxidant properties and reacts exclusively towards unsaturated organics via electrophilic or electron abstraction [3]. FFA (k_2 (FFA, $^1O_2$) = 1.2×10^9 $M^{-1}s^{-1}$) and NaN_3 (k_2 (NaN_3, $^1O_2$) = 1×10^9 $M^{-1}s^{-1}$) were therefore selected rather than the saturated compounds (e.g., MeOH) [5,18] to quench $^1O_2$ since PDS could not be directly decomposed by FFA and azide (Fig. S4a). The degradation kinetics of phenol was significantly reduced in presence of excess FFA (k_{obs} = 0.04 min^{-1}) and NaN_3 (k_{obs} = 0.02 min^{-1}) (Table 1). Besides, NaN_3 was further used as the chemical probe for $^1O_2$ generation, which manifested a higher second order rate of 1 x10^9 $M^{-1}s^{-1}$ than the targeted phenolic compound (2.0-3.0 $\times 10^6$ $M^{-1}s^{-1}$), but excess NaN_3 could only delay the removal of phenol (Fig. S4b), which suggested the involvement of $^1O_2$ in PDS/CuO system but excluded $^1O_2$ as a predominant reactive oxygen species for phenol degradation. The rapid physical quenching with water with a rate constant of $k_1 = 2.5 \times 10^5$ s^{-1} further explained this point [45]. To detect the occurrence of H_2O_2 due to further transformation of $O_2^{\bullet-}$, molybdate salt was used because this latter rapidly reacts with H_2O_2 to produce a peroxymolybdate complex, which can be easily detected by UV/Vis spectrophotometry at λ = 570 nm. As shown in Fig. S5, the adsorption for the peroxymolybdate

complex was detected in CuO alone, which indirectly proved that a minor amount of $^{\bullet}O_2^-$ was produced by oxygen reduction, while the majority of $^{\bullet}O_2^-$ was generated in the CuO/PDS system which was highlighted by a higher absorbance. These results thus confirmed the intermediate role of $^{\bullet}O_2^-$ during the generation of $^1O_2$. However, in the CuO/PDS system, $^{\bullet}O_2^-$ reaction with Cu^{2+} (k_2 = 8 x10^9 $M^{-1}s^{-1}$) was likely a more important sink of $^{\bullet}O_2^-$ than $^{\bullet}O_2^-$ bimolecular dismutation leading to Cu^+ generation. This result also discarded $^1O_2$ as the leading reactive oxygen species for phenol degradation.

Reactive species	Scavenger	Concentration (mM)	K_{obs} (min^{-1})	R^2
	none		0.32	0.99
$^{\bullet}OH$ and $SO_4^{\bullet-}$	methanol	4900	0.18	0.99
$^{\bullet}OH$ and $SO_4^{\bullet-}$	anisole	18.5	0.24	0.98
$^{\bullet}OH$	nitrobenzene	19.4	0.32	0.96
$^{\bullet}O_2^-$	*p*-benzoquinone	18.5	0	-
$^1O_2$	furfuryl alcohol	100	0.04	0.94
$^1O_2$	azide	100	0.02	0.98
Cu(I)	neocuproine	0.19	0.05	0.94
Cu(I)	hydroxylamine	0.06	0.40	0.96

Table 1. Apparent first-order degradation kinetic rate constants (K_{obs}) of phenol in presence of different scavengers.

Consequently, Cu(III) was assumed to be the working oxidant in the CuO/PDS process. To verify this hypothesis, periodate was added to the reactive medium as it was reported to be able to stabilize the labile Cu(III) species by forming a Cu(III)−periodate complex. This complex has a characteristic light absorbance at 415 nm [23]. Interestingly, significant absorbance at this wavelength was observed when periodate was added into CuO/PDS, while no absorbance was found for CuO and PDS alone (Fig. 3a). This result supported our hypothesis of the presence of Cu(III) in the CuO/PDS process but without knowing if Cu(III) was surface-bound or in solution.

To collect additional evidence for the involvement of Cu(III) in phenol transformation, different compounds were tested because Cu(III) is highly selective towards electron-rich compounds (e.g., benzotriazole) but not reactive to electron-deficient compounds (e.g., benzoic acid) [24]. As shown in Fig. 3b, benzotriazole were readily transformed with k_{obs} = 0.57 min^{-1} and benzoic acid was not degraded at all while salicylic acid and 4-hydroxybenzoic acid showed an intermediate behavior with k_{obs} = 0.09 min^{-1} and k_{obs} = 0.21 min^{-1}, respectively.

3.4 Phenol transformation pathways and mechanisms

Phenol transformation pathways were investigated by identifying phenol TPs following a suspect screening workflow in LC-HRMS. For this purpose, a database was made up of a list of possible TPs with their molecular formula, exact mass and structure (Table S2). This list was

established from a literature search of TPs of phenol formed during AOPs experiments. In a first step, TPs with intensities lower than 1 $x10^4$ cps, signal to noise ratios lower than 10, isotopic ratios higher than 10%, and mass accuracy errors higher than 5 ppm were eliminated. Following this approach, only TPs resulting from phenol polymerization were detected. The structure of the first one with a retention time (RT) = 11.6 min and a pseudo-molecular $[M-H]^-$ ion at m/z = 185.0597 was assigned to 4-phenoxyphenol (dimer) after deconvolution of the TIC of samples (Fig. 4) and injection of an analytical standard. This compound did not accumulate with time. The structure of the following TPs with a RT = 13.8 min and 14.5 min and a $[M-H]^-$ ion at m/z = 277.0859 (and a related fragment ion at m/z 185.0597) and 369.1127, respectively were assigned to a trimer and a tetramer of phenol, respectively (Fig. 4).

Catechol, HQ and BQ were reported as common TPs of phenol in radical and non-radical based PDS activation systems [46]. Available catechol analytical standard was injected in LC-HRMS but was never detected during degradation experiments. Since BQ and HQ could not be analyzed in MS due to a very poor response in electrospray mode of ionization, standard addition of BQ and HQ were performed in LC/UV analysis, with limits of detection below 0.1 mg/L. Fig. S6 and Fig. S7 show the lack of formation BQ and HQ during the degradation experiments. Consequently, the polymerization reaction was found to be the only main phenol transformation pathway probably through an one-electron oxidation process of phenol under Cu(III) reactivity. The peak area variations of detected TPs are shown in Fig. S8. The dimer only accounted for 3 % of the initial phenol concentration and the amount of trimer and tetramer could not be quantified as no standard was commercially available. A mass balance was also not reached because compounds corresponding to a high degree of polymerization of phenol probably precipitated in the reactive medium.

On the basis of the elucidated phenol transformation pathway and on the knowledge of the different involved reactive species (see section 3.2), a mechanism was suggested as depicted in Fig. 5. Similar to what was suggested for the MnO_2/PDS system [47], a metastable copper complex was most likely formed at the surface of the hydrous CuO micro-particles. This was a reasonable assumption since at neutral pH, the CuO surface is positively charged (pHpzc of 8-9 have been reported for CuO, [48]) and PDS is an anion calling for strong electrostatic interactions. As a result, the S-O bond of PDS weakened and broke (Eq. (1)) and the adsorption of PDS on the surface of CuO facilitated the generation of metastable $[\equiv Cu(III)-O-O-SO_3]$ intermediate. The latter resulting complex underwent hydrolysis along with the generation of $^{\bullet}O_2^-$ (see Eq. (2)). Afterward, the recombination of two $^{\bullet}O_2^-$ could evolve into $^1O_2$ with the concomitant release of H_2O_2 (Eq. (3)). However, most probably $^{\bullet}O_2^-$reacted with Cu(II) to generate Cu(I) (Eq. (4)) which could be spontaneously oxidized by PDS or H_2O_2 to give Cu(III) or Cu(II) (Eq. (5) - (7)). In turn, Cu(III) could selectively oxidize the electron-rich phenol to the corresponding phenoxyl radical leading to phenol polymerization, while it was reduced in Cu(II) (Eq. (8)) so that the catalytic effect involved alternate oxidation and reduction of copper. Phenol could be also oxidized by $^1O_2$ ($k_2 = 10^6$ $M^{-1}s^{-1}$, Eq. (9)) but this reaction was probably not significant due to $^1O_2$ physical quenching with water. In neutral solutions, $^{\bullet}OH$ is not an intermediate in the decomposition reaction of Cu(III), except when Cu(III) is not efficiently

consumed by organic compounds [25]. In our experiments, the Cu(III) ions seemed to oxidize phenol without a need for a complexation step of Cu(II) with the organic contaminant to enhance PDS activation as was observed in case of the antibiotic cephalexin [21].

$$[\equiv \mathrm{Cu(II)-OH}]^{\mathrm{I}} + \mathrm{S_2O_8^{2-}} \rightarrow [\equiv \mathrm{Cu(III)-O-O-SO_3}]^{\mathrm{I}} + \mathrm{e^-} + \mathrm{SO_4^{2-}} + \mathrm{H^+} \quad \text{Eq. (1)}$$

$$[\equiv \mathrm{Cu(III)-O-O-SO_3}]^{\mathrm{I}} + \mathrm{e^-} + 2\mathrm{H_2O} \rightarrow [\equiv \mathrm{Cu(II)-OH}\ ]^{\mathrm{I}} + {}^{\bullet}\mathrm{O_2^-} + \mathrm{SO_4^{2-}} + 3\mathrm{H^+} \quad \text{Eq. (2)}$$

$$2\,{}^{\bullet}\mathrm{O_2^-} + 2\mathrm{H_2O} \rightarrow {}^1\mathrm{O_2} + \mathrm{H_2O_2} + 2\mathrm{OH^-} \quad \text{Eq. (3)}$$

$$\mathrm{Cu(II)} + {}^{\bullet}\mathrm{O_2^-} \rightarrow \mathrm{Cu(I)} + \mathrm{O_2} \quad \text{Eq. (4)}$$

$$\mathrm{Cu(I)} + \mathrm{H_2O_2} \rightarrow \mathrm{Cu(III)} + 2\mathrm{OH^-} \quad \text{Eq. (5)}$$

$$\mathrm{Cu(I)} + \mathrm{S_2O_8^{2-}} \rightarrow \mathrm{Cu(III)} + 2\mathrm{SO_4^{2-}} \quad \text{Eq. (6)}$$

$$\mathrm{Cu(I)} + \mathrm{S_2O_8^{2-}} \rightarrow \mathrm{Cu(II)} + \mathrm{SO_4^{2-}} + \mathrm{SO_4^{\bullet -}} \quad \text{Eq. (7)}$$

$$\mathrm{Cu(III)} + \mathrm{Ph-OH} \rightarrow \mathrm{Cu(II)} + \mathrm{Ph-O^{\bullet}} + \mathrm{H^+} \quad \text{Eq. (8)}$$

$${}^1\mathrm{O_2} + \mathrm{Ph-OH} \rightarrow \mathrm{O_2} + \mathrm{Ph-O^{\bullet}} + \mathrm{H^+} \quad \text{Eq. (9)}$$

$^{\bullet}$OH and $SO_4^{\bullet -}$ radicals [19, 31, 32], CuO surface metastable complexes [11,17, 19] and $^1O_2$ [19] have been reported as the responsible reactive species for the degradation of organic compounds in the CuO/PDS system, differently, Cu(III) was proposed as the primary oxidant species in this study.

3.5 Influence of operating parameters

Solution pH. The solution pH can affect the surface charge property of CuO, the PDS activation and the dissociation and the degradation efficiency of phenol. The pH effect was firstly investigated at three different pH values (i.e., 4, 7 and 9). Neutral and alkaline conditions were obtained using Tris buffer, while acidic conditions were reached in distilled water through PDS decomposition. pH values were kept constant ($pH_0 \pm 0.2$) during the degradation experiments. The k_{obs} at different pH are reported in Fig. 6a, showing that degradation was faster at acidic and basic pH than at neutral pH.

Recent empirical evidence suggested that base-activated PDS must be conducted at pH > 10 to be effective [49] and this process did not therefore account for faster phenol degradation at pH 9. More plausibly, with a pKa of 10, a very small percentage of phenol appeared as phenolate ion which was much easily oxidized than the neutral phenol (k_{obs} = 0.53 min^{-1} vs k_{obs} = 0.32 min^{-1}). At acidic pH, Cu(III) readily decomposed into $^{\bullet}$OH which might explain a higher apparent kinetic rate constant (k_{obs} = 0.44 min^{-1}). To confirm this point, NB was applied in the CuO/PDS/phenol system. As shown in Fig. S9, NB had a stronger inhibitory effect on the phenol degradation under acidic condition than under neutral condition. This result also indirectly confirmed the generation of Cu(III) in CuO/PDS system since Cu(III) decomposed in $^{\bullet}$OH at acidic pH.

Water constituents. The influence of natural anions and dissolved organic matter (DOM) on phenol degradation was investigated separately. Cl^- and HCO_3^- are common background electrolytes in real water and they usually negatively influence the efficiency of radical-based AOPs as they are radical quenchers. In the CuO/PDS system, Cl^- (0.2 g/L) and HCO_3^- (0.5 g/L) anions had no significant influence on the phenol degradation (Table 2). These results confirmed earlier findings that Cu(III) was not very reactive towards Cl^- avoiding the formation of the chloride radicals (e.g., $Cl_2^{\bullet-}$) which are common to radical-based processes. The lack of Cl^- reactivity was confirmed by the lack of detection of 2-chlorophenol, 4-chlorophenol, and 2,4-dichlorophenol in LC-HRMS after injecting their analytical standards (Fig. S10). In homogeneous Cu^{2+}/PMS system, the negative role of HCO_3^- was ascribed to their coordination with Cu^{2+} [50]. This was not observed in CuO/PDS system most likely because most of the reactive Cu^{2+} ions were surface bound. Humic acids were also used as a surrogate for DOM at a concentration level of 2 mg/L, a value representative of DOM level in groundwater. In these conditions, the phenol degradation was only slightly inhibited (k_{obs} = 0.27 min^{-1} instead of k_{obs} = 0.32 min^{-1} in distilled water, Table 2) even though a competition of humic acids and phenol for the oxidant was expected. This small decrease in degradation was most likely due to adsorption of humic acid on the surface of the catalyst which could minimize the complexation of PDS on the catalyst surface.

Water constituent	K_{obs} (min^{-1})	R^2
Pure water	0.32	0.99
Cl^-	0.32	0.97
HCO_3^-	0.28	0.99
HA	0.27	0.96
SO_4^{2-}	0.07	0.99
Wastewater	0.11	0.96

Table 2. Water matrix effect on phenol degradation. [phenol] = 20 mg/L; [CuO] = 10 g/L; [PDS] = 1 mM; [Cl^-] = 200 mg/L; [HCO_3^-] = 500 mg/L; [SO_4^{2-}] = 500 mg/L; [Humic acids (HA)] = 2 mg/L; pH = 7 with Tris buffer.

More surprisingly, the CuO/PDS system was strongly blocked when sulfate anion concentrations were increased. This result meant that sulfate anions probably interacted with positively charged CuO blocking reactive sites for PDS activation. To confirm this specific point, different SO_4^{2-} concentrations were generated in the CuO/PDS system by varying the PDS concentrations used. Assuming that each mole of PDS led to two moles of SO_4^{2-}, 192, 96 and 38.4 mg/L of SO_4^{2-} were generated when adding 1, 0.5 and 0.2 mM of PDS, respectively. The results for phenol and PDS degradation are shown in Fig. 7a and Fig. 7b, respectively. Half-lives of PDS decreased from 15 min to 8 min in presence of 1 mM or 0.2 mM PDS, supporting the SO_4^{2-} sorption on catalyst surfaces as an inhibitory process for PDS decomposition. However, phenol degradation was much higher at 1 mM PDS (k_{obs} = 0.32 min^{-}

^{1}) than at 0.2 mM (k_{obs} = 0.02 min^{-1}), supporting that PDS decomposition was likely not the limiting step in phenol degradation kinetics.

Real wastewater. The investigated oxidation process was also applied for the treatment of a domestic wastewater treatment plant effluent spiked with 20 mg/L of phenol. The major physico-chemical properties of the wastewater are reported in Table S2. The phenol degradation was still effective with only a three-fold decrease in phenol half-lives when switching from distilled water to wastewater (k_{obs} = 0.11 min^{-1}, Table 2). The slower degradation was likely due to the competition of DOM (TOC =12.65 mg/L) for oxidant.

Cu leaching from CuO. The stability of the catalyst was assessed against the leached concentration of Cu measured in solution by ICP-AES after a filtration step on 0.45 µm cellulose filters. The Cu leaching from CuO in presence of PDS and phenol was investigated in different waters including distilled water (DW) at acidic (pH = 3.5) and neutral pH and in secondary treated domestic wastewater (WW, pH = 7.8). The results are shown in Fig. 6b. Surprisingly, the Cu leaching dramatically decreased when moving from distilled water at neutral pH (63.5 mg/L after 24 h reaction time) to wastewater (0.27 ± mg/L at the end of the 24 h reaction time). An unexpected result was a lower Cu leaching (47.3 mg/L after 24 h reaction time) at acidic pH in distilled water without a clear explanation for this experimental result. Moreover, the Cu release was not linearly correlated with the oxidant concentration since a Cu concentration value of 0.21 mg/L was reached at a PDS concentration of 0.1 mM which was close to the concentration obtained at 1 mM PDS (Table S3). The low Cu leaching in wastewater treatment might be ascribed to HCO_3^- and its complexing ability to Cu^{2+}. Indeed, in presence of 1-10 mM of HCO_3^-, Cu^{2+} may predominantly exist as surface insoluble $CuCO_3$ [50]. The Cu leaching was far less than that of 1 mg/L which is required by environmental quality standards for surface water and by drinking water regulations, making the CuO/PDS oxidation system promising in application. In addition, the CuO/PDS was still efficient in phenol removal with only a three-fold decrease in phenol half-lives when switching from distilled water to wastewater.

Stability and reusability. For a sustainable operation with high performance, the CuO particles need to maintain high catalytic activity and stable structure for prolonged operation time. Therefore, sequential experiments were carried out to investigate the reusability of CuO. After four cycles of CuO use, no significant deterioration in the catalytic activity was observed and the phenol degradation rates remained higher than 82% (Fig. 8a). Interestingly, compared with distilled water, the PDS decomposition was significantly limited in wastewater (Fig. 8b) and steadily decreased across the successive experiments (Fig. 8b), likely due to increased sorption of SO_4^{2-} anions and/or DOM on CuO active sited. A lower PDS activation led to catalyst preservation and calls for avoiding the PDS usage in excess.

3.6 Applicability of CuO/PDS system.

To evaluate the practical applicability of CuO/PDS system, we investigated the removal of several antibiotics namely SMX, CLA, CIP and CFX, belonging to several different families of environmental relevance (i.e., sulfonamide, macrolide, fluoroquinolone and cephalosporin, respectively) in distilled water. SMX, CLA, CIP and CFX were all degraded and degradation

kinetics fitted to a first order kinetic model with k_{obs} = 0.24 ± 0.02, 0.12 ± 0.01, 0.31 ± 0.03, 3.10 ± 0.22 min^{-1}, respectively. Their transformation pathways were elucidated by identifying their TPs following a suspect screening workflow in LC-HRMS (see Fig. 9). The databases were made up of a list of possible antibiotic TPs with their molecular formula and exact mass (Table S4 – S7). All detected TPs of target antibiotics with a mass error < 5 ppm are shown in Fig. S11 – S14 and were previously identified under different oxidative processes. Consequently, detailed interpretation of MS data is not presented. As shown in Fig. 9a, the CIP degradation could be due to the stepwise decomposition of the piperazine ring by Cu(III) through electron transfer at the secondary amine leading to ring opening and the generation of N-desethylene-CIP (CIP 2) by losses of a formaldehyde group from CIP 1. CIP 2 was further oxidized to CIP 3 through N-dealkylation reaction. This piperazine ring cleavage pathway has been previously reported under $SO_4^{\bullet-}$ oxidation. However, in contrast to $SO_4^{\bullet-}$, which is another well-known one-electron oxidant [51], the hydroxylation pathway with hydroxyl radical firstly attacking on the quinolone ring and the substitution of the fluorine atom by a hydroxyl group were not observed. As shown in Fig. 9b, two oxidation pathways were operating simultaneously for SMX degradation: (1) oxidation of the amine group through a one electron oxidation process to form a N-central radical, yielding to the generation of a dimer (SMX 1, m/z 503) and (2) cleavage of the sulfonamide bond leading to SMX 2 (m/z 174) and SMX 3 (m/z 99). In contrast to SMX degradation under $SO_4^{\bullet-}$ oxidation, hydroxylation of the benzene and isoxazole rings was not observed, neither was observed the formation of the nitro-SMX derivative which involved $^{\bullet}OH$ [52]. Three main TPs of CFX were detected: CFX 1 (m/z 364), CFX 2 (m/z 336) and CFX 3 (m/z 151). Under thermal activated persulfate, the formation of six isomers at m/z 364 was reported resulting from either oxygen transfer or hydroxylation processes [53]. Only one TP at m/z 364 was detected in CuO/PDS system. The formation of the sulfoxide derivative was the most reasonable pathway because this transformation was observed in presence of PDS alone. It was also shown that the complex of Cu^{2+} with CFX could efficiently activate PDS to induce rapid degradation of CFX [21] with CFX 2 generation, as the predominant TP. This transformation reaction most likely took place in CuO/PDS due to Cu^{2+} leaching and was ascribed to cupryl ion reactivity. CFX 2 resulted from a decarboxylation reaction of CFX 1. CFX 3 was likely to be evolved from a dealkylation reaction following single electron transfer at the N of the amide group. As shown in Fig. 9d, CLA underwent two transformation reactions including N-demethylation leading to CLA 1 (m/z 734) and O-dealkylation leading to cladinose and desosamine sugar losses, while the lactone ring was preserved. These N- and O-dealkylation reactions were most likely initiated by a one-electron oxidation of the heteroatom. Hydroxylation reactions, which were reported for the degradation of erythromycin under UV-C/PDS irradiation were not observed [54]. Collectively, the results of this work confirmed that Cu(III) is a strong one-electron oxidant due to its high reduction potential in solid (Cu(III)/Cu(II) = 2.3 V) and presented high reactivity against N and O containing electron rich moieties leading to the degradation of different classes of antibiotics. Higher Cu(III) selectivity than $SO_4^{\bullet-}$ was also observed, since hydroxylation reactions were avoided. $SO_4^{\bullet-}$oxidation and $^{\bullet}OH$ oxidation (resulting from $SO_4^{\bullet-}$decomposition) lead to the formation of 6-hydroxy-6-defluoro-CIP, 14-

hydroxy-CLA and 4-nitro-SMX. All these TPs preserve biological activity. Consequently, Cu(III) oxidant appeared to restrict the number of generated TPs of toxicological concern.

4. Conclusions

In this study, the CuO catalyzed PDS activation system was deeply investigated and presented high efficiency for phenol degradation in different waters including wastewater at neutral pH. Identification of reactive species and phenol TPs identification demonstrated that Cu(III) most likely acted as the predominant reactive species for phenol degradation. $^1O_2$, even though highly formed in the CuO/PDS system, was a minor contributor during the phenol degradation process due to physical quenching with water. Therefore, the CuO catalyzed PDS system showed great advantages for water treatment application as the high resistance to the background Cl^- anions without the formation of chlorinated by-products, with limited Cu^{2+} leaching (below 0.5 mg/L) and limited oxidant consumption in wastewater due to poor reactivity of Cu(III) with DOM. Cu(III) being an one-electron transfer oxidant, the system presented a preference to react with electron-rich compounds such as phenols leading to polymerization reactions. The efficient degradation of selected antibiotics by CuO/PDS system also demonstrated the practical applicability of this system for emerging contaminants removal. However, besides Cu(III), $^1O_2$ and Cu(I) were generated in the CuO/PDS. All these species are known to be good biocides which opens a possibility to use the CuO/PDS system for water disinfection.

Acknowledgements: This research was financially supported by the Water Joint Programming Initiative (JPI) through the research project IDOUM - Innovative Decentralized and low cost treatment systems for Optimal Urban wastewater Management. Chan Li thanks the Occitanie Region for her PhD grant.

References

[1] E.J. Behrman, Peroxydisulfate chemistry in the environmental literature : A brief critique, J. Hazard. Mater. 35 (2018) 0–1. https://doi.org/10.1016/j.jhazmat.2018.11.018.

[2] J. Wang, S. Wang, Activation of persulfate (PS) and peroxymonosulfate (PMS) and application for the degradation of emerging contaminants, Chem. Eng. J. 334 (2018) 1502–1517. https://doi.org/10.1016/j.cej.2017.11.059.

[3] J. Lee, U. Von Gunten, J.H. Kim, Persulfate-based advanced oxidation: Critical assessment of opportunities and roadblocks, Environ. Sci. Technol. 54 (2020) 3064–3081. https://doi.org/10.1021/acs.est.9b07082.

[4] S. Wacławek, H. V Lutze, K. Grübel, V.V.T. Padil, M. Černík, D.D. Dionysiou, Chemistry of persulfates in water and wastewater treatment: A review, Chem. Eng. J. 330 (2017) 44–62. https://doi.org/10.1016/j.cej.2017.07.132.

[5] A. Jawad, K. Zhan, H. Wang, A. Shahzad, Z. Zeng, J. Wang, X. Zhou, H. Ullah, Z. Chen, Z. Chen, Tuning of persulfate activation from a free radical to a nonradical pathway through the incorporation of non-redox magnesium oxide, Environ. Sci. Technol. 54 (2020) 2476–2488. https://doi.org/10.1021/acs.est.9b04696.

[6] J. Yan, J. Li, J. Peng, H. Zhang, Y. Zhang, B. Lai, Efficient degradation of sulfamethoxazole by the CuO @ Al2O3 (EPC) coupled PMS system : Optimization , degradation pathways and toxicity evaluation, Chem. Eng. J. 359 (2019) 1097–1110. https://doi.org/10.1016/j.cej.2018.11.074.

[7] Y. Leng, W. Guo, X. Shi, Y. Li, A. Wang, F. Hao, L. Xing, Degradation of Rhodamine B by persulfate activated with Fe3O4: Effect of polyhydroquinone serving as an electron shuttle, Chem. Eng. J. 240 (2014) 338–343. https://doi.org/10.1016/j.cej.2013.11.090.

[8] R. Li, X. Jin, M. Megharaj, R. Naidu, Z. Chen, Heterogeneous Fenton oxidation of 2,4-dichlorophenol using iron-based nanoparticles and persulfate system, Chem. Eng. J. 264 (2015) 587–594. https://doi.org/10.1016/j.cej.2014.11.128.

[9] A. Jawad, J. Lang, Z. Liao, A. Khan, J. Ifthikar, Z. Lv, S. Long, Z. Chen, Z. Chen, Activation of persulfate by CuOx@Co-LDH: A novel heterogeneous system for contaminant degradation with broad pH window and controlled leaching, Chem. Eng. J. 335 (2018) 548–559. https://doi.org/10.1016/j.cej.2017.10.097.

[10] F. Ji, C. Li, L. Deng, Performance of CuO / Oxone system : Heterogeneous catalytic oxidation of phenol at ambient conditions, Chem. Eng. J. 178 (2011) 239–243. https://doi.org/10.1016/j.cej.2011.10.059.

[11] T. Zhang, Y. Chen, Y. Wang, J. Le Roux, Y. Yang, J.P. Croué, Efficient peroxydisulfate activation process not relying on sulfate radical generation for water pollutant degradation, Environ. Sci. Technol. 48 (2014) 5868–5875.

https://doi.org/10.1021/es501218f.

[12] Y. Ding, H. Tang, S. Zhang, S. Wang, H. Tang, Efficient degradation of carbamazepine by easily recyclable microscaled CuFeO2 mediated heterogeneous activation of peroxymonosulfate, J. Hazard. Mater. 317 (2016) 686–694. https://doi.org/10.1016/j.jhazmat.2016.06.004.

[13] Y. Xu, J. Ai, H. Zhang, The mechanism of degradation of bisphenol A using the magnetically separable CuFe2O4 / peroxymonosulfate heterogeneous oxidation process, J. Hazard. Mater. 309 (2016) 87–96. https://doi.org/10.1016/j.jhazmat.2016.01.023.

[14] S. Wang, J. Tian, Q. Wang, F. Xiao, S. Gao, W. Shi, F. Cui, Development of CuO coated ceramic hollow fiber membrane for peroxymonosulfate activation: a highly efficient singlet oxygen-dominated oxidation process for bisphenol a degradation, Appl. Catal. B Environ. 256 (2019) 117783. https://doi.org/10.1016/j.apcatb.2019.117783.

[15] Copper in drinking water, Background document for development of WHO guidelines for drinking-water quality (2004). https://www.who.int/water_sanitation_health/dwq/chemicals/copper.pdf.

[16] L.R. Bennedsen, J. Muff, E.G. Søgaard, Influence of chloride and carbonates on the reactivity of activated persulfate, Chemosphere. 86 (2012) 1092–1097. https://doi.org/10.1016/j.chemosphere.2011.12.011.

[17] X. Du, Y. Zhang, I. Hussain, S. Huang, W. Huang, Insight into reactive oxygen species in persulfate activation with copper oxide : Activated persulfate and trace radicals, Chem. Eng. J. 313 (2017) 1023–1032. https://doi.org/10.1016/j.cej.2016.10.138.

[18] S. Wang, S. Gao, J. Tian, Q. Wang, T. Wang, X. Hao, F. Cui, A stable and easily prepared copper oxide catalyst for degradation of organic pollutants by peroxymonosulfate activation, J. Hazard. Mater. 387 (2020) 121995. https://doi.org/10.1016/j.jhazmat.2019.121995.

[19] S. Xing, W. Li, B. Liu, Y. Wu, Y. Gao, Removal of ciprofloxacin by persulfate activation with CuO : A pH-dependent mechanism, Chem. Eng. J. 382 (2020) 122837. https://doi.org/10.1016/j.cej.2019.122837.

[20] Y. Yang, G. Banerjee, G.W. Brudvig, J.H. Kim, J.J. Pignatello, Oxidation of organic compounds in water by unactivated peroxymonosulfate, Environ. Sci. Technol. 52 (2018) 5911–5919. https://doi.org/10.1021/acs.est.8b00735.

[21] J. Chen, X. Zhou, P. Sun, Y. Zhang, C. Huang, Complexation enhances Cu(II)-activated peroxydisulfate: A novel activation mechanism and Cu(III) contribution, Environ. Sci. Technol. 53 (2019) 11774–11782. https://doi.org/10.1021/acs.est.9b03873.

[22] Y.N. Ogibin, I. Troyanskii, E.K. Starostin, S.I. Moryasheva, G.I. Nikishin, Participation of Cu(III) in copper sulfqte-catalyzed oxidation of 3-carboxypropyl radicals with

S2O82- ions, Bull. Acad. Sci. USSR, Div. Chem. Sci. 26 (1977) 859–862. https://doi.org/10.1007/bf01108221.

[23] L. Wang, H. Xu, N. Jiang, Z. Wang, J. Jiang, T. Zhang, Trace cupric species triggered decomposition of peroxymonosulfate and degradation of organic pollutants: Cu(III) being the primary and selective intermediate oxidant, Environ. Sci. Technol. 54 (2020) 4686–4694. https://doi.org/10.1021/acs.est.0c00284.

[24] Y. Feng, W. Qing, L. Kong, H. Li, D. Wu, Y. Fan, Factors and mechanisms that in fluence the reactivity of trivalent copper : A novel oxidant for selective degradation of antibiotics, Water Res. 149 (2019) 1–8. https://doi.org/10.1016/j.watres.2018.10.090.

[25] D. Meyerstein, Trivalent copper. I. A pulse radiolytic study of the chemical properties of the aquo complex, Inorg. Chem. 10 (1971) 638–641. https://doi.org/10.1021/ic50097a040.

[26] L.W. Matzek, K.E. Carter, Activated persulfate for organic chemical degradation : A review, Chemosphere. 151 (2016) 178–188. https://doi.org/10.1016/j.chemosphere.2016.02.055.

[27] Z. Chen, Q. Wan, G. Wen, X. Luo, X. Xu, J. Wang, K. Li, T. Huang, J. Ma, Effect of borate buffer on organics degradation with unactivated peroxymonosulfate: Influencing factors and mechanisms, Sep. Purif. Technol. 256 (2021) 117841. https://doi.org/10.1016/j.seppur.2020.117841.

[28] C. Liang, C.F. Huang, N. Mohanty, R.M. Kurakalva, A rapid spectrophotometric determination of persulfate anion in ISCO, Chemosphere. 73 (2008) 1540–1543. https://doi.org/10.1016/j.chemosphere.2008.08.043.

[29] E. Graf, J.T. Penniston, Method for determination of hydrogen peroxide, with its application illustrated by glucose assay., Clin. Chem. 26 (1980) 658–660. https://doi.org/10.1093/clinchem/26.5.658.

[30] S. V. Lapshin, V.G. Alekseev, Copper(II) complexation with ampicillin, amoxicillin, and cephalexin, Russ. J. Inorg. Chem. 54 (2009) 1066–1069. https://doi.org/10.1134/S0036023609070122.

[31] H. Liang, Y. Zhang, S. Huang, I. Hussain, Oxidative degradation of p-chloroaniline by copper oxidate activated persulfate, Chem. Eng. J. 218 (2013) 384–391. https://doi.org/10.1016/j.cej.2012.11.093.

[32] Y. Cho, R. Lin, Y. Lin, Science of the total evironment degradation of 2, 4-dichlorophenol by CuO-activated peroxydisulfate : Importance of surface-bound radicals and reaction kinetics, Sci. Total Environ. 699 (2020) 134379. https://doi.org/10.1016/j.scitotenv.2019.134379.

[33] C.L. Clifton, R.E. Huie, Rate constants for hydrogen abstraction reactions of the sulfate

radical , SO4- . alcohols, Int. J. Chem. Kinet. 21 (1989) 677–687. https://doi.org/10.1002/kin.550210807.

[34] J. Hu, H. Dong, J. Qu, Z. Qiang, Enhanced degradation of iopamidol by peroxymonosulfate catalyzed by two pipe corrosion products (CuO and Δ-MnO2), Water Res. 112 (2017) 1–8. https://doi.org/10.1016/j.watres.2017.01.025.

[35] D.B. Fenn, M.M. Mortland, T.J. Pinnavaia, The chemisorption of anisole on Cu(II) hectorite, Clays Clay Miner. 21 (1973) 315–322. https://doi.org/10.1346/CCMN.1973.0210507.

[36] P. O'Neill, S. Steenken, D. Schulte-Frohlinde, Formation of radical cations of methoxylated benzenes by reaction with OH radicals, Ti 2+ , Ag 2+ , and SO 4.- in aqueous solution. An optical and conductometric pulse radiolysis and in situ radiolysis electron spin resonance study, J. Phys. Chem. 79 (1975) 2773–2779. https://doi.org/10.1021/j100592a013.

[37] R.G. Zepp, J. Holgne, H. Bader, Nitrate-induced photooxidation of trace organic chemicals in water, Environ. Sci. Technol. 21 (1987) 443–450. https://doi.org/10.1021/es00159a004.

[38] L.M. Dorfman, G.E. Adams, Reactivity of the hydroxyl radical in aqueous solutions, 1973. https://doi.org/10.6028/nbs.nsrds.46.

[39] P. Neta, V. Madhavan, H. Zemel, R.W. Fessenden, Rate constants and mechanism of reaction of SO4·- with aromatic compounds, J. Americn Chem. Soc. 99 (1977) 163–164. https://doi.org/10.1021/ja00443a030.

[40] M. Hicks, J.M. Gebicki, Rate constants for reaction of hydroxyl radicals with Tris, Tricine and Hepes buffers, FEBS Lett. 199 (1986) 92–94. https://doi.org/10.1016/0014-5793(86)81230-3.

[41] A. B.Ross, P. Neta, Rate constants for reactions of inorganic radicals in aqueous solution, Vol. 65. Washington, DC: US Department of Commerce, National Bureau of Standards. (1979). https://doi.org/10.6028/nbs.nsrds.65.

[42] B.H.J. Bielski, D.E. Cabelli, Superoxide and hydroxyl radical chemistry in aqueous solution, in: Act. Oxyg. Chem., 1995: pp. 66–104. https://doi.org/10.1007/978-94-007-0874-7_3.

[43] Y. Tsujimoto, H. Hashizume, M. Yamazaki, Superoxide radical scavenging activity of phenolic compounds, Int. J. Biochem. 25 (1993) 491–494. https://doi.org/10.1016/0020-711X(93)90655-X.

[44] H. Lee, H. Lee, J. Seo, H. Kim, Y.K. Shin, J. Kim, C. Lee, Activation of oxygen and hydrogen peroxide by copper(II) coupled with hydroxylamine for oxidation of organic contaminants, Environ. Sci. Technol. 50 (2016) 8231–8238.

https://doi.org/10.1021/acs.est.6b02067.

[45] F.E. Scully Jr., J. Hoigné, Rate constants for reactions of singlet oxygen with phenols and other compounds in water, Chemosphere. 16 (1987) 681–694. https://doi.org/10.1016/0045-6535(87)90004-x.

[46] T. Olmez-hanci, I. Arslan-alaton, Comparison of sulfate and hydroxyl radical based advanced oxidation of phenol, Chem. Eng. J. 224 (2013) 10–16. https://doi.org/10.1016/j.cej.2012.11.007.

[47] S. Zhu, X. Li, J. Kang, X. Duan, S. Wang, Persulfate activation on crystallographic manganese oxides : Mechanism of singlet oxygen evolution for nonradical selective degradation of aqueous contaminants, Environ. Sci. Technol. 53 (2019) 307–315. https://doi.org/10.1021/acs.est.8b04669.

[48] M. Ghulam, T. Hajira, S. Muhammad, A. Nasir, Synthesis and characterization of cupric oxide (CuO) nanoparticles and their application for the removal of dyes, African J. Biotechnol. 12 (2013) 6650–6660. https://doi.org/10.5897/ajb2013.13058.

[49] O.S. Furman, A.L. Teel, R.J. Watts, Mechanism of base activation of persulfate, Environ. Sci. Technol. 44 (2010) 6423–6428. https://doi.org/10.1021/es1013714.

[50] L. Cheng, M. Wei, L. Huang, F. Pan, D. Xia, X. Li, A. Xu, Efficient H2O2 oxidation of organic dyes catalyzed by simple copper(II) ions in bicarbonate aqueous solution, Ind. Eng. Chem. Res. 53 (2014) 3478–3485. https://doi.org/10.1021/ie403801f.

[51] N.S. Shah, J. Ali Khan, M. Sayed, Z. Ul Haq Khan, H. Sajid Ali, B. Murtaza, H.M. Khan, M. Imran, N. Muhammad, Hydroxyl and sulfate radical mediated degradation of ciprofloxacin using nano zerovalent manganese catalyzed S2O82−, Chem. Eng. J. 356 (2019) 199–209. https://doi.org/10.1016/j.cej.2018.09.009.

[52] M. Mahdi Ahmed, S. Barbati, P. Doumenq, S. Chiron, Sulfate radical anion oxidation of diclofenac and sulfamethoxazole for water decontamination, Chem. Eng. J. 197 (2012) 440–447. https://doi.org/10.1016/j.cej.2012.05.040.

[53] Y. Qian, G. Xue, J. Chen, J. Luo, X. Zhou, P. Gao, Q. Wang, Oxidation of cefalexin by thermally activated persulfate: Kinetics, products, and antibacterial activity change, J. Hazard. Mater. 354 (2018) 153–160. https://doi.org/10.1016/j.jhazmat.2018.05.004.

[54] I. Michael-Kordatou, M. Iacovou, Z. Frontistis, E. Hapeshi, D.D. Dionysiou, D. Fatta-Kassinos, Erythromycin oxidation and ERY-resistant Escherichia coli inactivation in urban wastewater by sulfate radical-based oxidation process under UV-C irradiation, Water Res. 85 (2015) 346–358. https://doi.org/10.1016/j.watres.2015.08.050.

Figure captions

Fig. 1. (a) SEM image and (b) XRD pattern of the investigated micro-sized copper oxide.

Fig. 2. (a) Phenol degradation and (b) PDS decomposition in PDS alone, CuO alone, Cu^{2+} solution, Cu^{2+}/PDS and CuO/PDS systems. [CuO] = [CuSO4.5H2O] = 10 g/L; [PDS] = 1 mM; [phenol] = 20 mg/L; pH = 7 with Tris buffer.

Fig. 3. (a) UV-Vis absorbance spectra of CuO/PDS after the addition of periodate for Cu(III) detection at pH 13, (b) degradation of selected compounds in CuO/PDS systems. [CuO] = 10 g/L; [PDS] = 1 mM; [KIO_4] = 4 g/L; [benzoic acid] = [benzotriazole] = [salicylic acid] = [4-hydroxybenzoic acid] = 20 mg/L.

Fig. 4. Extracted Ion Chromatograms (EIC) of detected phenol transformation products.

Fig. 5. Scheme of phenol transformation mechanisms in CuO/PDS system.

Fig. 6. (a) Degradation kinetic rate constants of phenol at different solution pH and (b) the effect of water matrix on copper ion leaching. The WW was filtered (0.45 μm) before adding CuO, PDS and phenol. [CuO] = 10 g/L; [PDS] = 1 mM; [phenol] = 20 mg/L.

Fig. 7. Effect of PDS concentration on degradation kinetics of (a) phenol and (b) PDS in CuO/PDS system at pH = 7 using TRIS buffer. [CuO] = 10 g/L; [PDS] = 0.2, 0.5 and 1 mM; [phenol] = 20 mg/L.

Fig. 8. (a) Phenol degradation and (b) PDS decomposition kinetics across four sequential experiments. [CuO] = 10 g/L; [PDS] = 1 mM; [phenol] = 20 mg/L. Every treatment cycle lasted 60 min.

Fig. 9. Proposed transformation pathways of (a) ciprofloxacin (CIP), (b) sulfamethoxazole (SMX), (c) cephalexin (CFX) and (d) clarithromycin (CLA) in the CuO/PDS system.

(a)

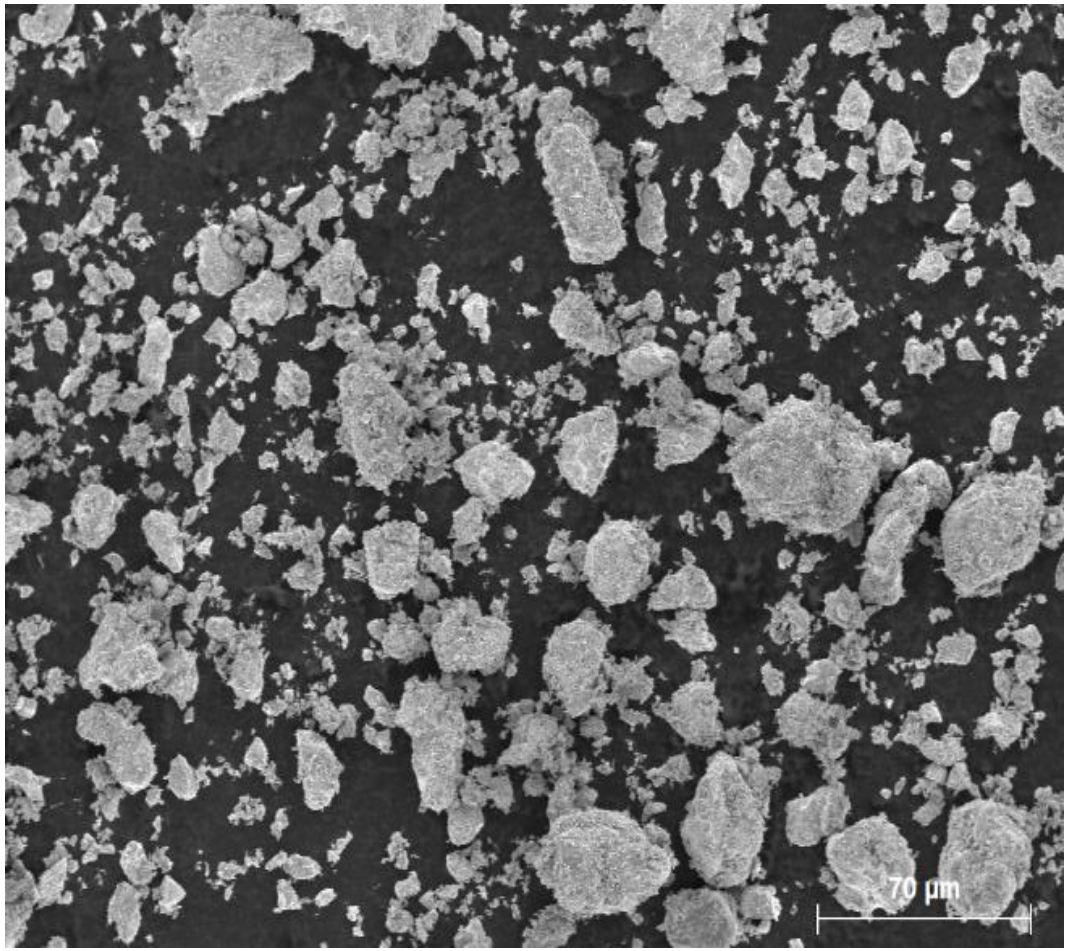
70 µm

(b)

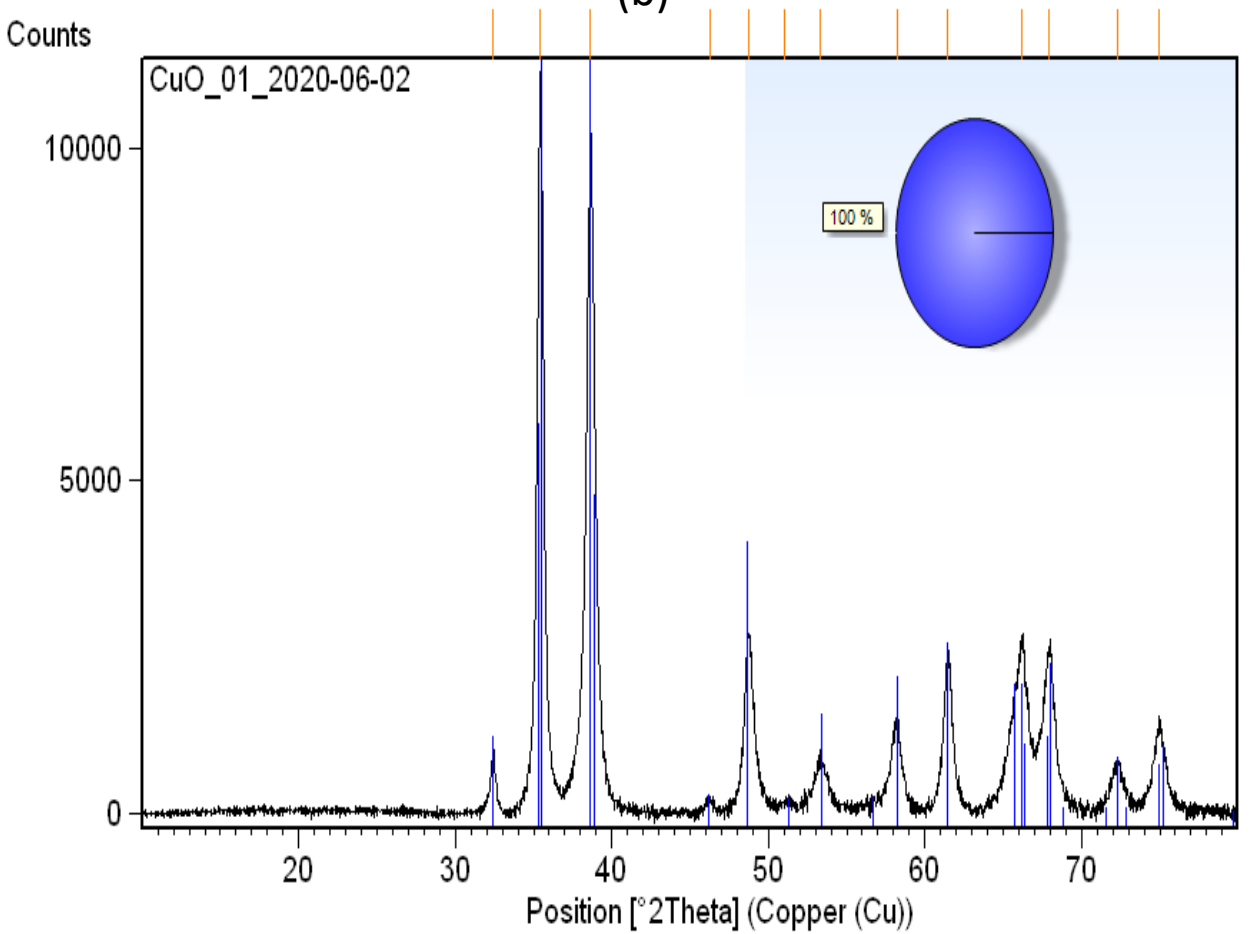
Counts
CuO_01_2020-06-02
10000
5000
0
100 %
20
30
40
50
60
70
Position [°2Theta] (Copper (Cu))

FIGURE 1

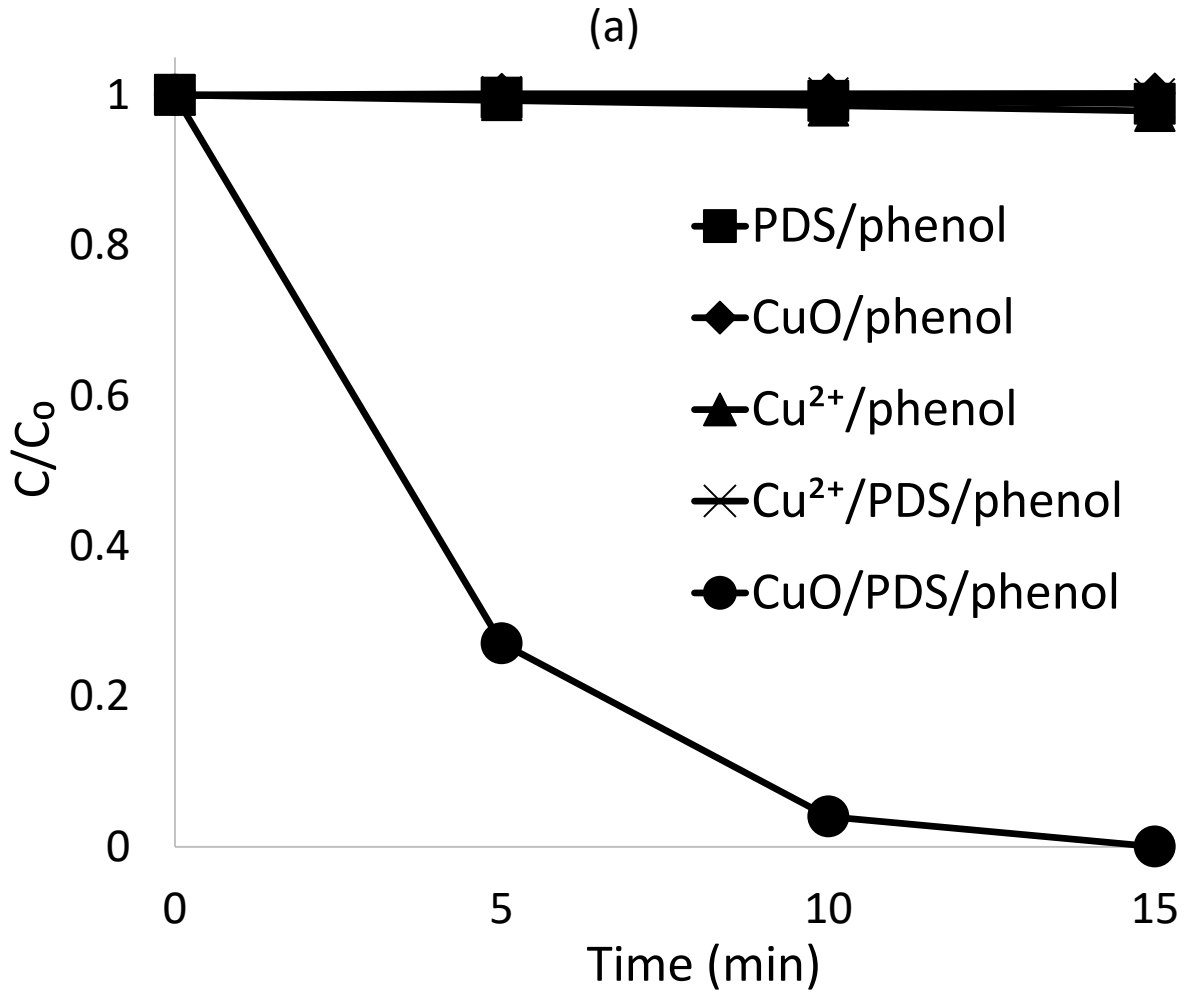
(a)
1
0.8
0.6
0.4
0.2
0
C/C0
0
5
10
15
Time (min)
PDS/phenol
CuO/phenol
Cu2+/phenol
Cu2+/PDS/phenol
CuO/PDS/phenol

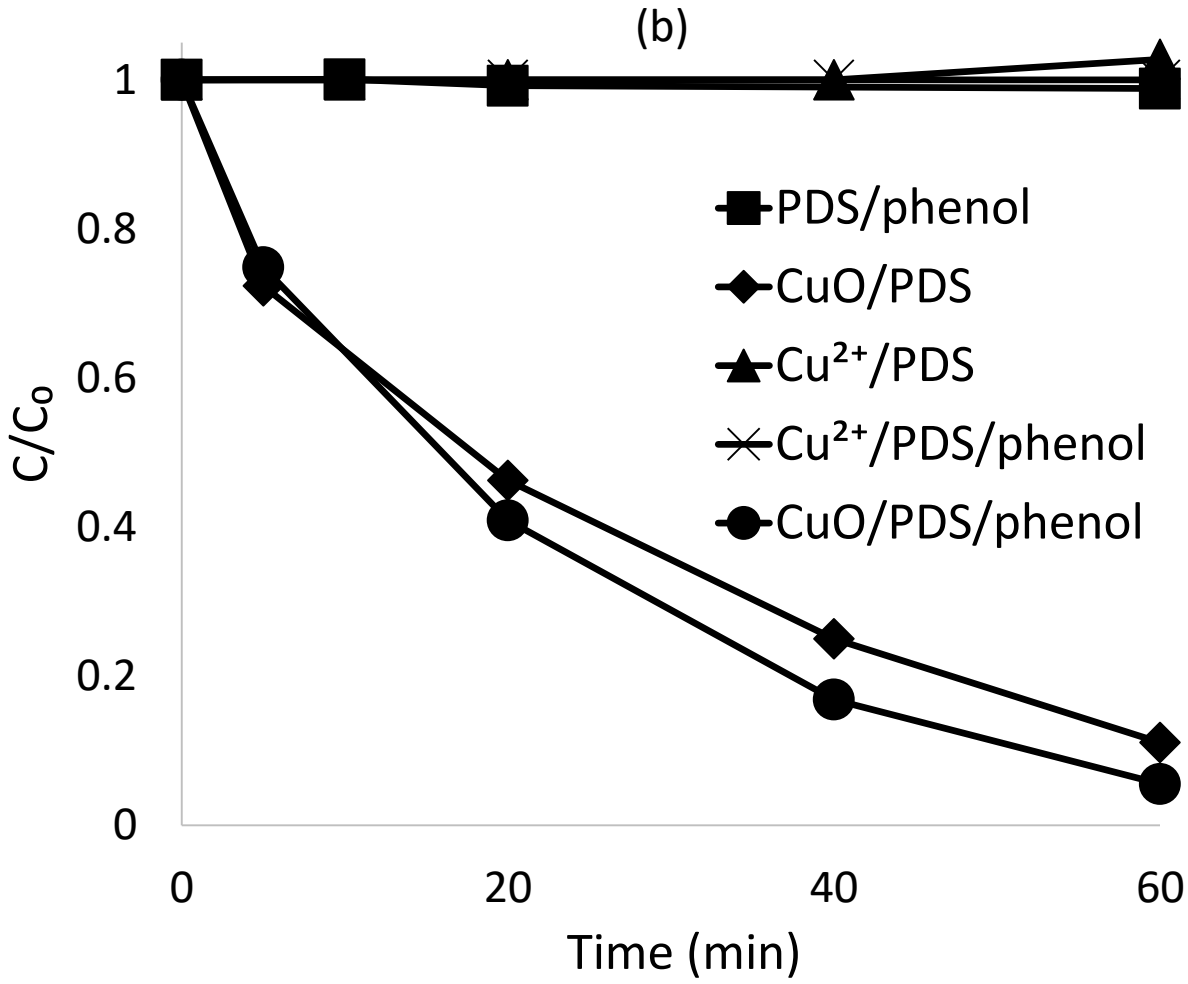
(b)
1
0.8
0.6
0.4
0.2
0
C/C0
0
20
40
60
Time (min)
PDS/phenol
CuO/PDS
Cu2+/PDS
Cu2+/PDS/phenol
CuO/PDS/phenol

FIGURE 2

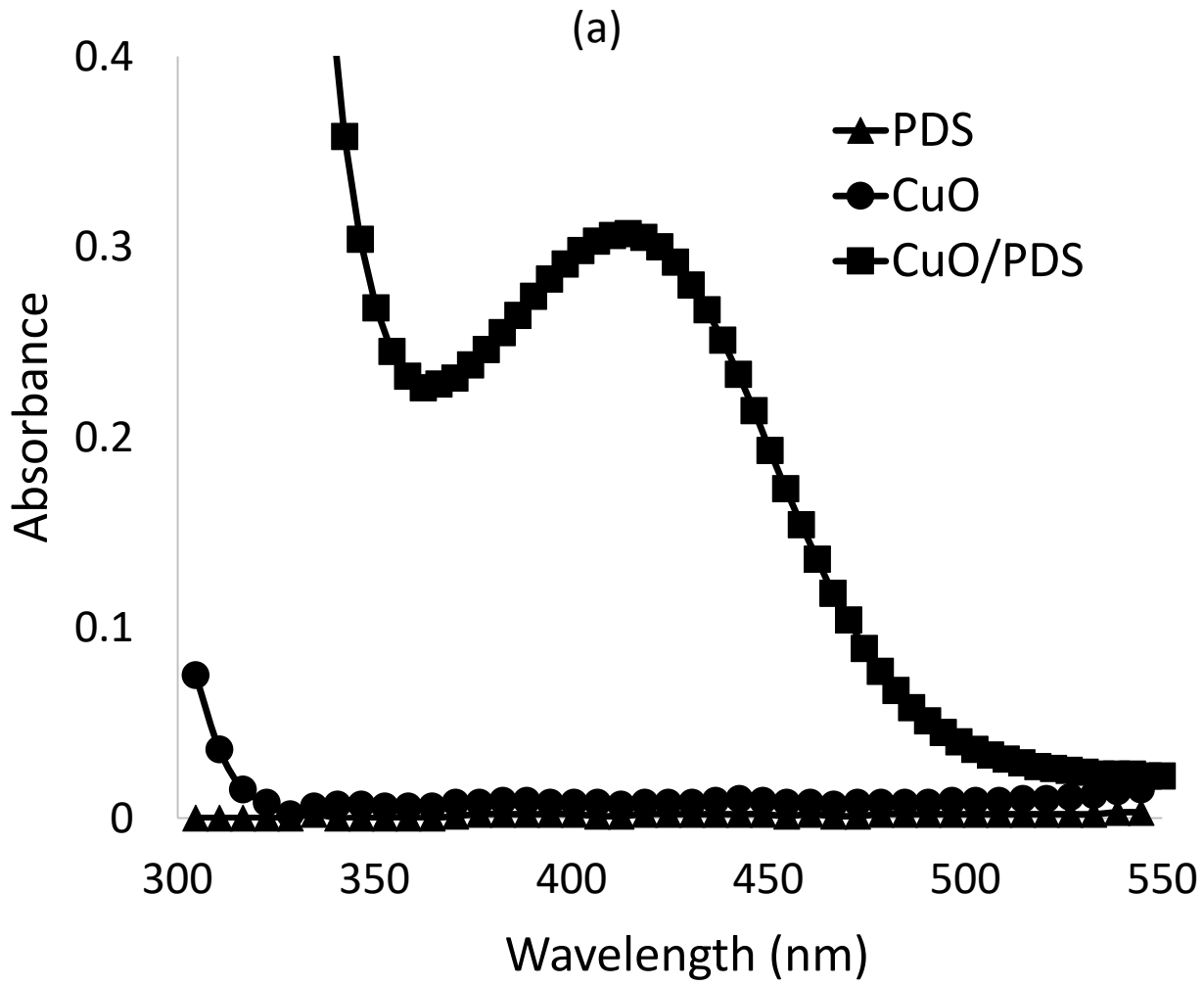
(a)
Absorbance
Wavelength (nm)
PDS
CuO
CuO/PDS
0.4
0.3
0.2
0.1
0
300
350
400
450
500
550

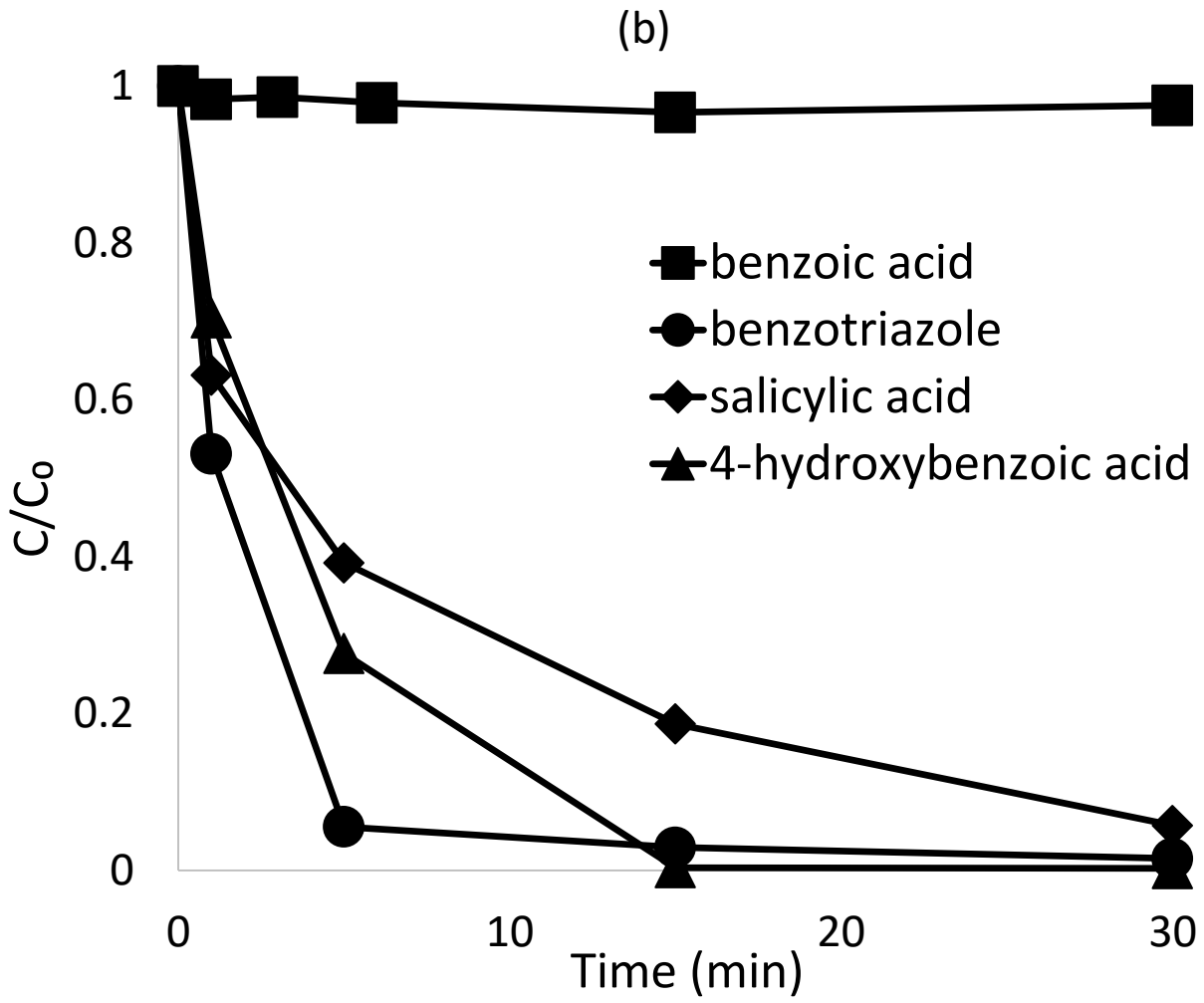
(b)
C/C0
Time (min)
benzoic acid
benzotriazole
salicylic acid
4-hydroxybenzoic acid
1
0.8
0.6
0.4
0.2
0
0
10
20
30

FIGURE 3

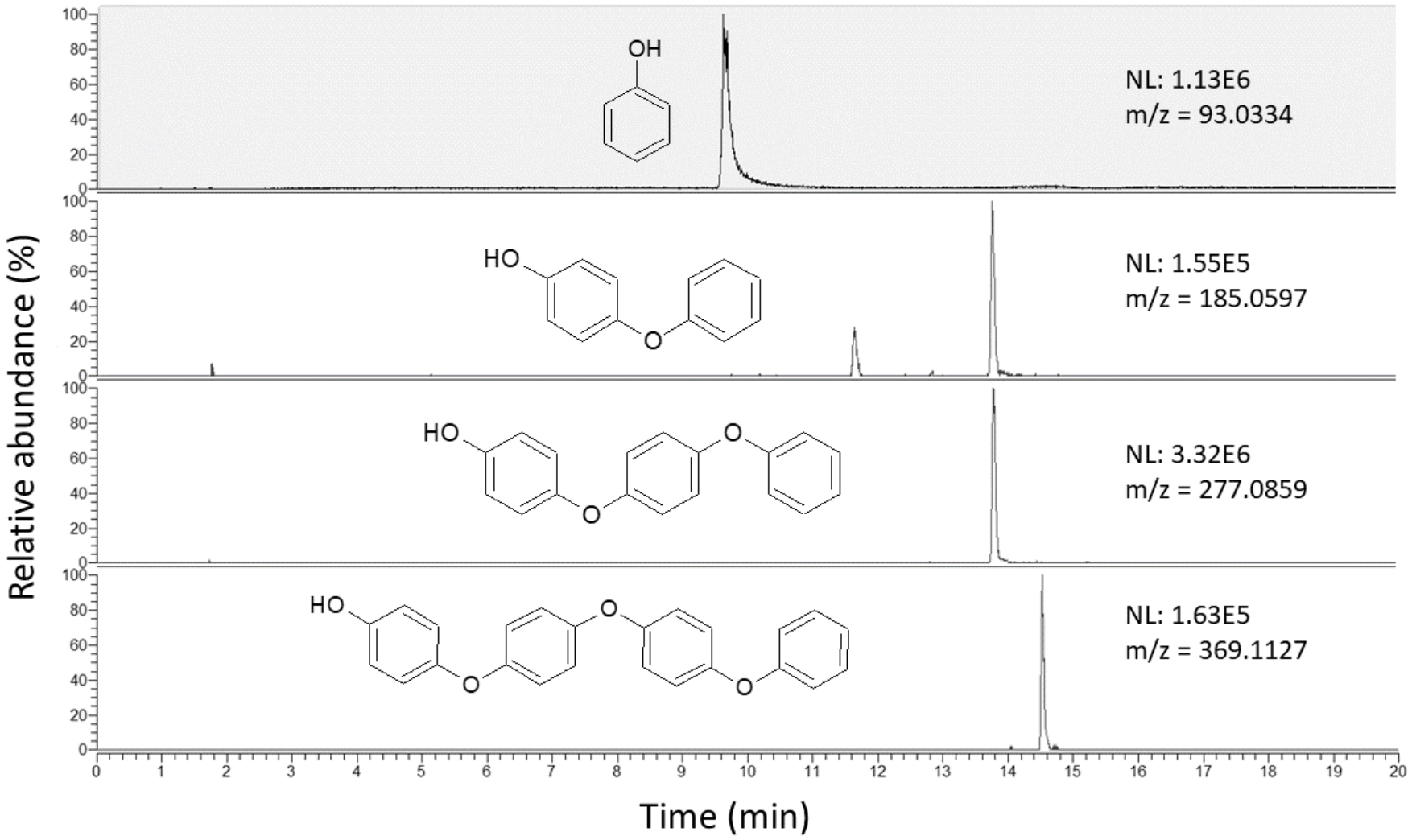
Relative abundance (%)
Time (min)
NL: 1.13E6
m/z = 93.0334
NL: 1.55E5
m/z = 185.0597
NL: 3.32E6
m/z = 277.0859
NL: 1.63E5
m/z = 369.1127
OH
HO
O

FIGURE 4

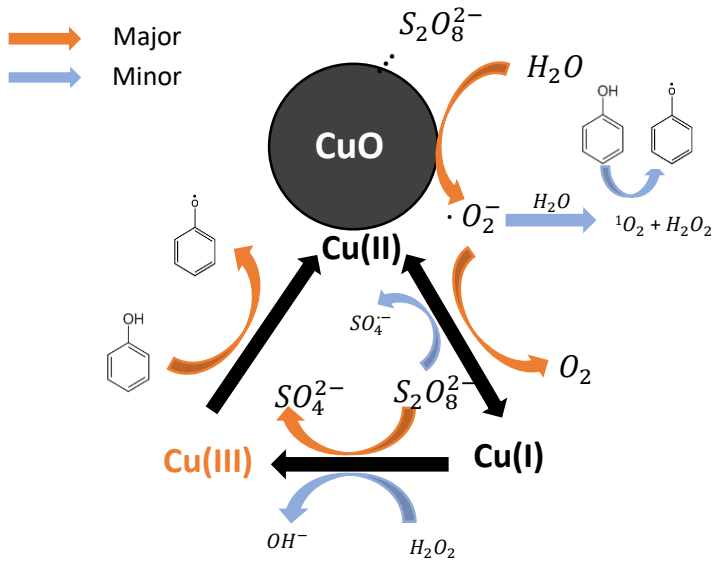
Major
Minor
$S_2O_8^{2-}$
CuO
H_2O
OH
$\cdot O_2^-$
H_2O
$^1O_2 + H_2O_2$
Cu(II)
OH
$SO_4^{\cdot-}$
O_2
SO_4^{2-}
$S_2O_8^{2-}$
Cu(III)
Cu(I)
OH^-
H_2O_2

FIGURE 5

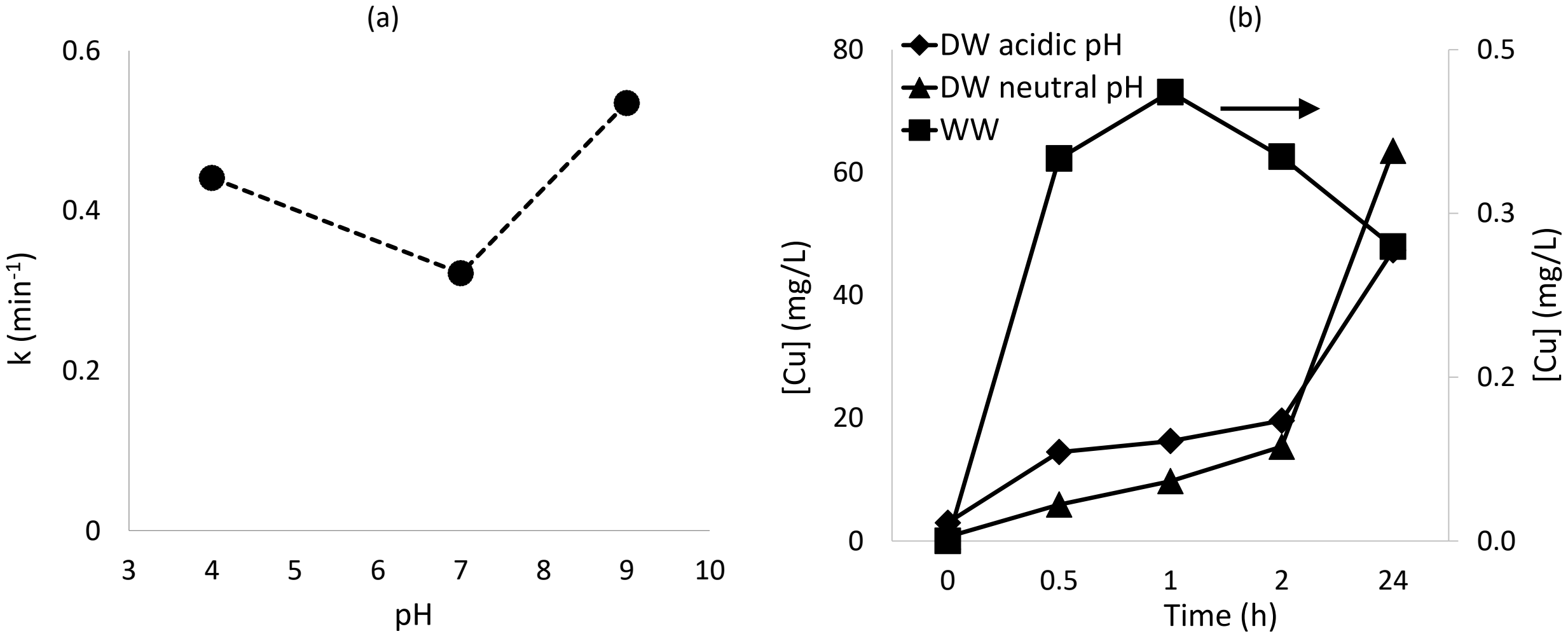
(a)
0.6
0.4
0.2
0
k (min-1)
3
4
5
6
7
8
9
10
pH
(b)
DW acidic pH
DW neutral pH
WW
80
60
40
20
0
[Cu] (mg/L)
0.5
0.3
0.2
0.0
[Cu] (mg/L)
0
0.5
1
2
24
Time (h)

FIGURE 6

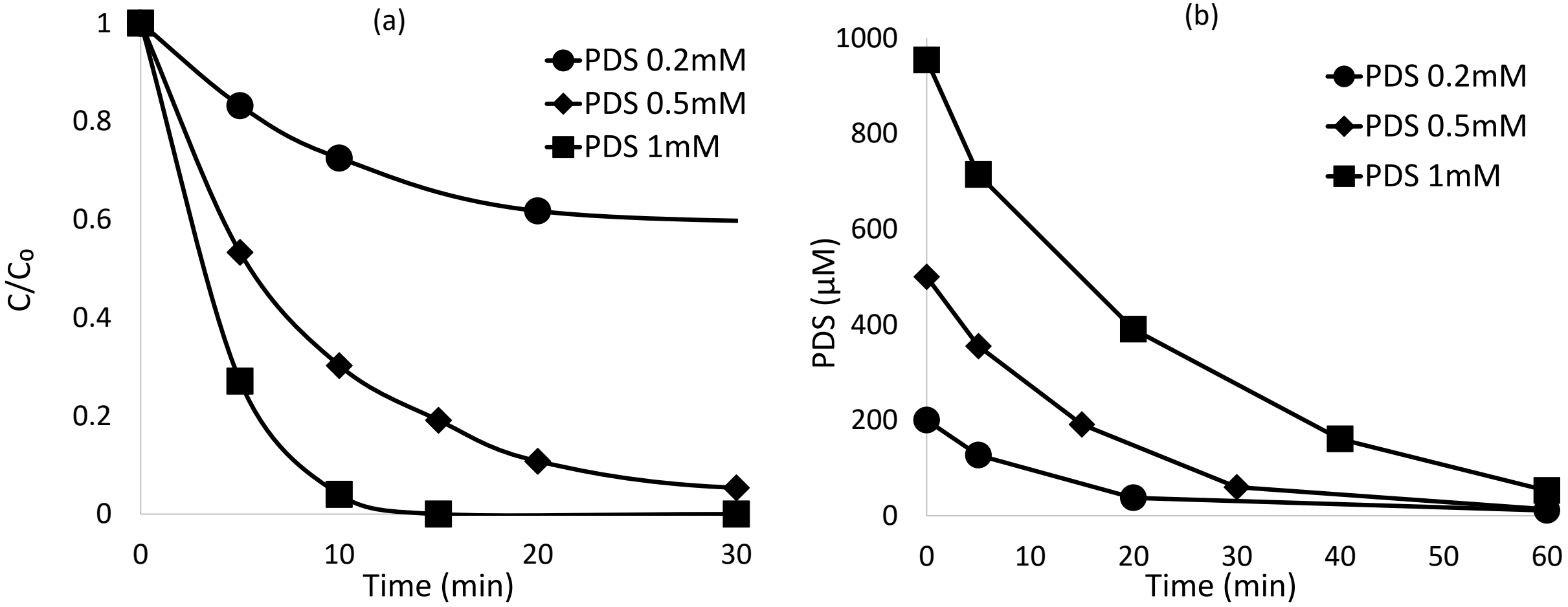
(a)
1
0.8
0.6
0.4
0.2
0
C/C0
0
10
20
30
Time (min)
PDS 0.2mM
PDS 0.5mM
PDS 1mM
(b)
1000
800
600
400
200
0
PDS (µM)
0
10
20
30
40
50
60
Time (min)
PDS 0.2mM
PDS 0.5mM
PDS 1mM

FIGURE 7

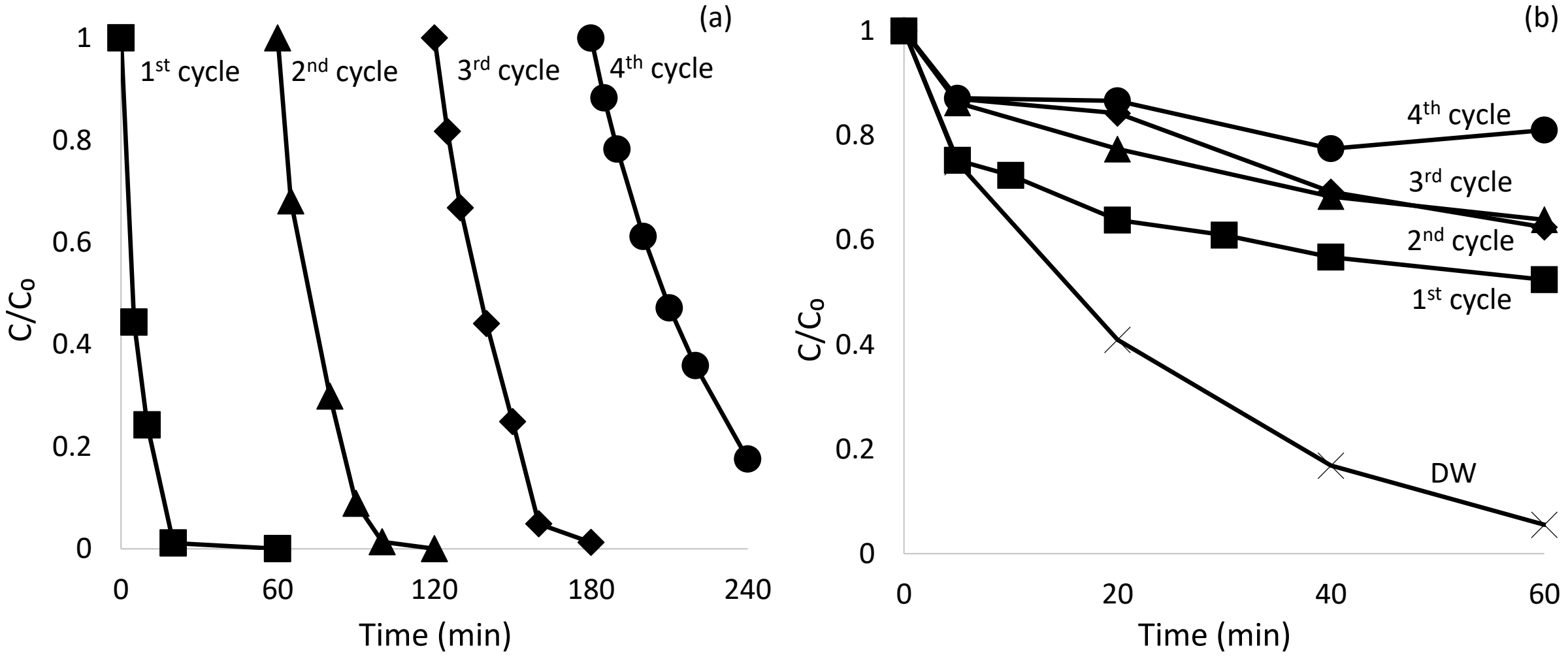
(a)
1st cycle
2nd cycle
3rd cycle
4th cycle
C/C0
Time (min)
(b)
4th cycle
3rd cycle
2nd cycle
1st cycle
DW
C/C0
Time (min)

FIGURE 8

FIGURE 9

(a)

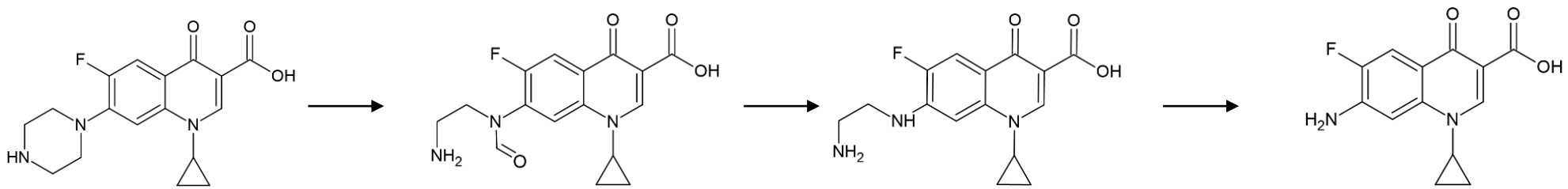

CIP
m/z 332

CIP 1
m/z 334

CIP 2
m/z 306

CIP 3
m/z 263

(b)

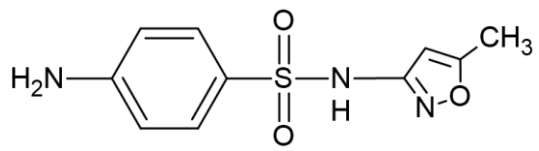

SMX
m/z 254

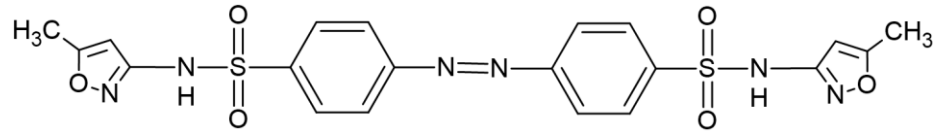

SMX 1
m/z 503

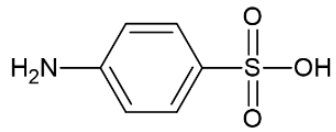

SMX 2
m/z 174

+

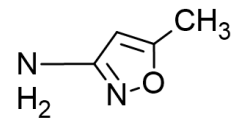

SMX 3
m/z 99

(c)

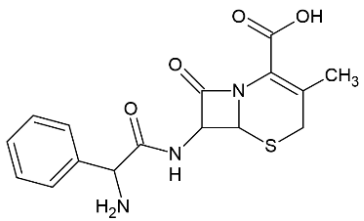

CFX
m/z 348

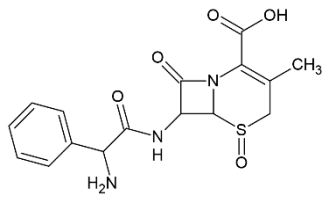

CFX 1
m/z 364

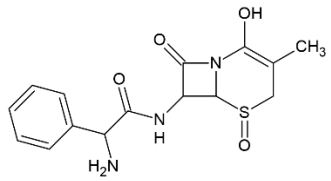

CFX 2
m/z 336

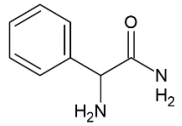

CFX 3
m/z 151

(d)

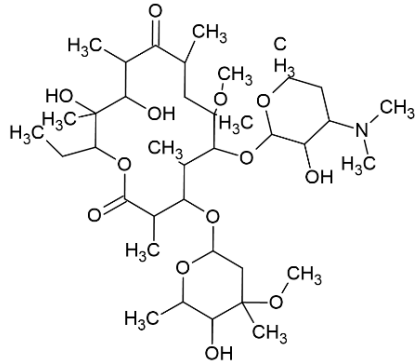

CLA
m/z 748

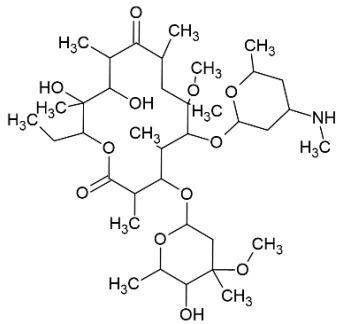

CLA 1
m/z 734

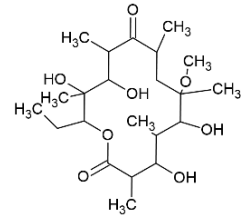

CLA 2
m/z 433